

## Distribution Agreement

In presenting this thesis or dissertation as a partial fulfillment of the requirements for an advanced degree from Emory University, I hereby grant to Emory University and its agents the non-exclusive license to archive, make accessible, and display my thesis or dissertation in whole or in part in all forms of media, now or hereafter known, including display on the world wide web. I understand that I may select some access restrictions as part of the online submission of this thesis or dissertation. I retain all ownership rights to the copyright of the thesis or dissertation. I also retain the right to use in future works (such as articles or books) all or part of this thesis or dissertation.

Signature:

---

Chen Chen

---

Date

Present and Potential Future Contributions of Ship Emissions to Air Quality and Human Health in  
the Pearl River Delta (PRD) region, China

By

Chen Chen  
Master of Science

Environmental Sciences

---

Dr. Eri Saikawa  
Advisor

---

Dr. Lance Gunderson  
Committee Member

---

Dr. Lance Waller  
Committee Member

Accepted:

---

Lisa A. Tedesco, Ph.D.  
Dean of the James T. Laney School of Graduate Studies

---

Date

Present and Potential Future Contributions of Ship Emissions to Air Quality and Human Health in  
the Pearl River Delta (PRD) region, China

By

Chen Chen  
B.S.M.A.S. (Hons) in Marine Science and Chemistry  
University of Miami  
2016

Advisor: Dr. Eri Saikawa

An abstract of  
A thesis submitted to the Faculty of the  
James T. Laney School of Graduate Studies of Emory University  
in partial fulfillment of the requirements for the degree of  
Master of Science  
in Environmental Sciences  
2018

## Abstract

### Present and Potential Future Contributions of Ship Emissions to Air Quality and Human Health in the Pearl River Delta (PRD) region, China

By Chen Chen

Ship emissions have been found to contribute to air pollution, potentially increasing the adverse health impacts of people living in coastal cities. I estimated the impacts caused by ship emissions, both on air quality and human health, in the present (2015) and future (2030) within the Pearl River Delta (PRD) region, China. In addition, I assessed the potential health benefits from implementing the Emission Control Area (ECA) policy in the region by predicting the avoided mortality, compared to the Business As Usual (BAU) scenario.

The PRD is a highly populated area with over 85 million people in 2015. Also, as one of the biggest port clusters in the world, 11.3, 89.5 and 141.9 kt/yr of PM<sub>2.5</sub>, SO<sub>2</sub> and NO<sub>x</sub>, respectively, are emitted within the 200 nautical mile (nm) coastline region. I found that these emissions increased PM<sub>2.5</sub> concentrations and O<sub>3</sub> mixing ratios by 1.1 µg/m<sup>3</sup> and 1.62 ppb, respectively, within the PRD. The health impacts from the ship emissions should not be neglected as about 155 and 115 excess acute mortality incidences are expected due to ship-related PM<sub>2.5</sub> and O<sub>3</sub> increase, respectively. Chronic mortality was more significant with 2,349 and 994 mortality incidences due to ship-related PM<sub>2.5</sub> and O<sub>3</sub>, respectively.

In 2030, I projected the future ship emissions under the BAU and ECA scenarios. I predicted 84% reductions for SO<sub>2</sub> and 13% for NO<sub>x</sub> emissions if ECA was implemented and found that this could avoid 1,044 and 143 deaths compared to the BAU scenario. The ship-induced mortality for PM<sub>2.5</sub> and O<sub>3</sub> would be reduced by 68% and 14% respectively if ECA was implemented, with a net reduction of 47% for the two pollutants combined. The health impacts due to ship emissions are non-negligible and an ECA implementation in the PRD region could notably prevent significant mortality.

Present and Potential Future Contributions of Ship Emissions to Air Quality and Human Health in  
the Pearl River Delta (PRD) region, China

By

Chen Chen  
B.S.M.A.S. (Hons) in Marine Science and Chemistry  
University of Miami  
2016

Advisor: Dr. Eri Saikawa

A thesis submitted to the Faculty of the  
James T. Laney School of Graduate Studies of Emory University  
in partial fulfillment of the requirements for the degree of  
Master of Science  
in Environmental Sciences  
2018

## **ACKNOWLEDGMENTS**

I give my greatest thanks to my dearest advisor Dr. Eri Saikawa, for her meticulous mentorship and guidance, and I also thank Dr. Lance Gunderson and Dr. Lance Waller for serving as committee members for my master thesis. I thank Dr. Alexander Avramov for guidance on meteorological analysis and programming, and Dr. Min Zhong for guidance on the air quality modeling. I also thank Antoinette Williams for reviewing and commenting on my thesis.

I also give thanks to all my marine team members in the International Council on Clean Transportation (ICCT), Dr. Bryan Comer, Ms. Xiaoli Mao and Dr. Dan Rutherford, for assisting me on the thesis and data acquisition. I thank Dr. Kathrine Walker and Dr. Allison Patton from the Health Effect Institute (HEI) for assisting on health benefits estimation and providing essential baseline mortality data. Lastly, thanks to Mr. Hongyang Cui and Dr. Qiang Zhang for providing the land emission data.

## Table of Contents

1. Introduction .....	1-5
2. Methodology .....	5-20
2.1. Study Flow Chart .....	5-5
2.2. Research area .....	6-7
2.3. Air quality simulations .....	7-11
2.4. Ship Emissions .....	11-17
2.5. Emission Scenarios .....	17-18
2.6. Ship Impacts .....	18-18
2.7. Health Impacts Estimation .....	18-21
2.8. Technical Support .....	21-21
3. Results .....	21-29
3.1. Emissions .....	21-23
3.2. Model Evaluation .....	23-24
3.3. Air Quality Impacts .....	24-26
3.4. Health Impacts .....	26-29
4. Discussion .....	29-35
5. Conclusion .....	35-36
6. References .....	37-41
7. Tables .....	42-52
7.1. Table 1 .....	42
7.2. Table 2 .....	43
7.3. Table 3 .....	44
7.4. Table 4 .....	45
7.5. Table 5 .....	46
7.6. Table 6 .....	47
7.7. Table 7 .....	48-49
7.8. Table 8 .....	50
7.9. Table 9 .....	51
7.10. Table 10 .....	52
8. Figures .....	53-65
8.1. Figure 1 .....	53
8.2. Figure 2 .....	54
8.3. Figure 3 .....	55
8.4. Figure 4 .....	56
8.5. Figure 5 .....	57
8.6. Figure 6 .....	58
8.7. Figure 7 .....	59
8.8. Figure 8 .....	60
8.9. Figure 9 .....	61
8.10. Figure 10 .....	62
8.11. Figure 11 .....	63
8.12. Figure 12 .....	64
8.13. Figure 13 .....	65
9. Supplementary Document.....	66-72
9.1. Table S1 .....	66
9.2. Table S2 .....	67
9.3. Table S3 .....	68
9.4. Table S4 .....	69
9.5. Table S5 .....	70
9.6. Table S6 .....	71
9.7. Table S7 .....	72



## List of abbreviations and acronyms

AIS	Automatic Identification System
BAU	Business as Usual
BC	Black Carbon
BR	Bohai Sea Rim
CARB	California Air Resources Board
CEV	Cerebrovascular Disease
CFC	Chlorofluorocarbon
COPD	Chronic Obstructive Pulmonary Disease
DECA	Domestic Emission Control Area
DESA	UN Department of Economic and Social Affairs
ECA	Emission Control Area
EEDI	Energy Efficiency Design Index
EF	Emission Factor
EU	European Union
FC	Fuel Consumption
FINN	Fire Inventory
GPW	Gridded Population of the World
HFO	Heavy Fuel Oil
HTAP	Task Force Hemispheric Transport of Air Pollution
ICCT	International Council on Clean Transportation
IER	Integrated Exposure Response
IHD	Ischemic Heart Disease
IMO	International Maritime Organization
LC	Lung Cancer
MADE/SORGAM	Model Aerosol Dynamics for Europe With the Secondary Organic Aerosol Model
MARPOL	The International Convention for the Prevention of Pollution from Ships
MDO	Marine Diesel Oil
MEGAN	Model of Emissions of Gases and Aerosols from Nature
MEIC	Multi-Resolution Emission Inventory of China
MFB	Mean Fractional Bias
MFE	Mean Fractional Error
MGO	Marine Gas Oil
MOT	Ministry of Transports
MOZART-4	Model for Ozone and Related Chemical Tracers
NCDC	National Climatic Data Center

NCEP	National Center for Environmental Prediction
NMB	Normalized Mean Bias
NME	Normalized Mean Error
NMVOG	Non-Methane Volatile Organic Compound
NOAA	National Oceanic and Atmospheric Administration
NO <sub>x</sub>	Nitrogen Oxides
O <sub>3</sub>	Tropospheric Ozone
OC	Organic Carbon
PM	Particulate Matter
PRD	Pearl River Delta
R	Correlation Coefficient
RADM2	Regional Acid Deposition Model Version 2
REAS	Regional Emission Inventory in Asia Version 2
RMSE	Root Mean Square Error
RR	Relative Risk
SAVE	Systematic Assessment of Vessel Emission Model
SCR	Selective Catalytic Reduction
SF	Scale Factor
SFOC	Specific Fuel Oil Consumption
SOA	Secondary Organic Aerosol
SO <sub>x</sub>	Sulfur Oxides
TEU	Twenty-Foot Equivalent Unit
UN ESCAP	United Nations Economic and Social Commission for Asia and the Pacific
VOC	Volatile Organic Carbon
WRF-Chem	Weather Research and Forecasting Coupled with Chemistry
YRD	Yangtze River Delta

## 1. Introduction

Exposure to particulate matter (PM), especially fine PM with an aerodynamic diameter less than or equal to 2.5  $\mu\text{m}$  ( $\text{PM}_{2.5}$ ), causes significant adverse health effects (EPA, 2009; WHO, 2013). Exposure to tropospheric ozone ( $\text{O}_3$ ) also poses an increased risk of death (Jerrett et al., 2009). Ship emissions are a major source of primary  $\text{PM}_{2.5}$ , including specific aerosols such as black carbon (BC), organic carbon (OC), as well as  $\text{O}_3$  precursors, including volatile organic compounds (VOC), and other gaseous pollutants such as sulfur oxides ( $\text{SO}_x = \text{SO}$  and  $\text{SO}_2$ ) and nitrogen oxides ( $\text{NO}_x = \text{NO}$  and  $\text{NO}_2$ ). The VOC and  $\text{NO}_x$  can react in the atmosphere in the presence of sunlight and form  $\text{O}_3$  (Eyring et al. 2010).

Shipping is an efficient and low-cost means of transportation. Shipping contributes to economic growth in foreign trade, especially in port cities (Frankel, 1989). Shipping transport has seen a steady increase (except 2009, the last financial crisis), owing to globalization and an increasing size of global-scale trade (UNCTAD, 2017). In 2015, over ten billion tons of goods (80% of global freights) were exchanged through seaborne trade worldwide (UNCTAD, 2017).

As a result of increased shipping, the local air quality in the coastal cities has deteriorated, partly due to ship emissions. Previous studies have found that ship emissions worsened the near-port ambient air quality. According to Corbett et al. (2007), nearly 70% of the ship's exhaust emissions occur within 400 km from the coastline. Other studies found a 1 - 45% increase of local  $\text{PM}_{2.5}$  concentrations due to ship emissions (Viana et al., 2009; Yau et al., 2013; Liu et al., 2016; Jeong et al., 2017; Zhang et al., 2017; Tao et al., 2017; Chen, 2018). Studies also revealed that ship emissions have non-negligible impacts on human health (Corbett et al., 1999; Corbett et al., 2007; Eyring et al., 2010; Tian et al., 2013; Sofiev et al., 2018). Corbett et al. (2007)

estimated that ship-related PM<sub>2.5</sub> were responsible for 60,000 cardiopulmonary and lung cancer deaths worldwide in 2002. Campling and Janssen et al. (2013) found that O<sub>3</sub> pollution due to oceangoing ships caused 2.6% of non-accidental premature deaths in the European Union (EU) Member States in 2005.

According to a recent greenhouse gas study, Smith et al. (2015) expect global trade, by shipping, will continue to increase in the future. Without effective emission control policies targeting oceangoing vessels, ship emissions will continue to grow in the future. To minimize both the adverse air pollution and health effects from ships, a series of local and global emission control standards have been implemented. The International Convention for the Prevention of Pollution from Ships (MARPOL) Annex VI by the International Maritime Organization (IMO) was the first large-scale emission control policy for ships adopted in 1997 and revised in 2008. It limits major pollutant emissions from ships, such as SO<sub>x</sub> and NO<sub>x</sub>, VOCs and other stratospheric ozone depleting substances, including halons and a number of chlorofluorocarbons (CFCs). Emission Control Areas (ECAs) were also established under MARPOL Annex VI to further limit sulfur contents of the fuel in the coastal areas, restricting ships to only use fuel with lower than 0.1% sulfur content after 2015. The current ECAs are located in the Baltic Sea and the North Sea. The North American ECAs, within 200 nautical miles (nm) of the North American coastline including Canada, also regulate NO<sub>x</sub> emission limits for the newly constructed ships. Local policies have further strengthened the emission limits, especially on coastal regions. California Air Resources Board (CARB), for example, require container ships to utilize shore power while at berth starting from 2008 (CARB, 2014). CARB recently also approved the use of an emission-capturing system as an alternative to shore power at the Port of Los Angeles (CARB, 2015). In the EU, similar actions are ongoing, including enlarging the current ECA

ranges and establishing a third ECA in the Mediterranean Sea. These policies aim to minimize ship emissions and provide health benefits to the associated areas.

Several studies have assessed the potential health benefits from the aforementioned ship emissions reduction policies. Winebrake et al., (2009) estimated that 33,500 premature deaths could be prevented annually, worldwide, if low-sulfur fuel (< 0.5% sulfur content) was used by ships in coastal regions instead of high sulfur content fuels (> 2.5%). Sofiev et al. (2018) predicted that the cleaner marine fuels (< 0.5%) could reduce ship-related premature mortality and morbidity by 34% and 54%, respectively in 2020, compared to 3.5% sulfur content fuels. These studies showed that an efficient control policy could render significant health benefits in the global domain.

China, as the world's largest product exporter, has substantial air quality and health risks associated with ship emissions as well. China owns nearly 5,000 ships with a total capacity of over 160 million tons and handled approximately one quarter of the world throughput in its container ports in 2015 (MOT, 2016). The three biggest port clusters in China are the Pearl River Delta (PRD), the Yangtze River Delta (YRD) and the Bohai Sea Rim (BR). The PRD port cluster, located in southern China (Figure 1), handled roughly 39% of all exports from China in 2015 (China Ports Yearbook, 2016). The PRD port cluster has 11 major ports and three of them, Shenzhen, Hong Kong and Guangzhou ports, are all ranked among the top ten largest container ports in the world (WSC, 2014). At the same time, over 58 million residents lived in the central PRD region in 2015 (GDstats, 2016) and two megacities, Guangzhou and Shenzhen, had over 13 and 11 million residents, respectively. Therefore, the emissions from oceangoing ships would pollute the local air quality and also risk the health conditions of local residents.

Many studies examined the impact of ship emissions on the local air quality in the coastal cities of China (Zhang et al., 2017; Chen et al., 2018; Liu et al., 2018; Lv et al., 2018) and a few also analyzed their potential health impacts. Liu et al. (2016) found that ship emissions in East Asia resulted in 14,500–37,500 premature deaths per year. In the PRD region, although there is no existing analysis that has included both acute and chronic mortality due to ship emissions, Lin et al. (2018) showed that ship emissions were an important factor of increased cardiovascular mortality in Guangzhou. Hence, efficient ship emission control policies are urgent for China to curtail the emissions within the coastal regions.

In 2015, the Chinese Ministry of Transports (MOT) implemented the Domestic Emission Control Area (DECA), which is similar but less stringent than the IMO ECA. DECA limits the sulfur contents of the fuels to less than 0.5% within the 12 nm offshore. The PRD region, the YRD and the BR are the three major port clusters under the DECA standard. According to MOT, SO<sub>x</sub> and PM emissions from ships in the three DECA regions would be reduced by 65% and 30% by 2020, respectively, compared to 2015 levels. However, due to its less stringent limitations, compared to the IMO ECA, DECA could be less effective in mitigating air pollution and thus allowing for higher mortality rates than ECA. To encourage the Chinese government to also apply the IMO ECA and better control ship emissions in China, it is necessary to assess the additional benefits that the ECA would bring along with the current DECA policy. To date, a limited number of studies have thoroughly explored the potential benefits that an IMO standard ECA could provide to the coastal cities in China.

The objectives of this study are to estimate the impacts caused by ship emissions on both air quality and human health, at present (2015) and in the future (2030) within the PRD region. With the 2015 data, I intend to identify the contributions of ship emissions to the ambient pollutant concentrations based on historical emissions and estimate ship-associated mortality from both acute and chronic exposures. I will also project the future ship emissions by 2030 under both Business As Usual (BAU) and Emission Control Area (ECA) scenarios. Lastly, I will assess the potential health benefits for the PRD region by 2030 with ECA implementation by predicting the avoided mortality compared to the BAU scenario. Based on the decreased ambient pollutant concentrations from the ECA scenario, my hypothesis is that the ECA implementation will have a significant impact on the reduction of ship emissions and associated mortality.

## **2. Methodology**

### **2.1. Study Flow Chart**

The thesis has three parts: Part 1 Emissions, Part 2 Modeling, and Part 3 Health Impact (Figure 1). For Part 1, I acquired and analyzed baseline emissions and estimated current and possible future ship emissions. For Part 2, I ran the air quality model under four scenarios: baseline and with ship scenarios in 2015, as well as BAU and ECA scenarios in 2030. Lastly, for Part 3, I estimated the ship-related mortality in 2015 and predicted the avoided mortality due to ECA in 2030 based on the modeled results.

### **2.2. Research Area**

The research area of this study is the entire PRD region, including the major cities, Guangzhou, Shenzhen, Dongguan, Foshan, Zhongshan, Zhuhai, Jiangmen, Zhaoqing, Huizhou, Macao and Hong Kong (Figure 1). These cities share similar geographical and cultural characteristics. The

PRD region is a subtropical-monsoon influenced humid climate, featuring a wet and hot summer and a dry and warm winter (Huang et al., 2012). The average temperature of spring, summer, fall, and winter in the PRD is approximately 20 °C, 28 °C, 25 °C and 12 °C, respectively. The monthly average rainfall is 250-300 mm during the rainy season from April to September. The monthly average precipitation in the dry season from October to February is approximately 50 mm.

In the PRD, the highest seasonal average PM<sub>2.5</sub> was observed in winter (80 µg/m<sup>3</sup>) and the season with the lowest concentration was in summer and spring (30 µg/m<sup>3</sup>) (Tao et al., 2017). Due to the accumulating attention from local governments, the annual average PM<sub>2.5</sub> concentration has been reduced from 79 µg/m<sup>3</sup> in 2007 to 46 µg/m<sup>3</sup> in 2016 (Guangdong-Hong Kong-Macao Pearl River Delta Regional Air Quality Monitoring Network, 2017).

On the other hand, the annual average ground-level O<sub>3</sub> mixing ratio increased from 24 ppb in 2006 to 29 ppb in 2014 (Guangdong-Hong Kong-Macao Pearl River Delta Regional Air Quality Monitoring Network, 2014). The concentrations of O<sub>3</sub> in downwind rural areas are usually higher than those in the urban areas. The highest daily maximum 8-hour average concentrations of O<sub>3</sub> are found in the summer from June to August and the lowest concentrations are found in the winter from December to February.

In 2015, over 58 million residents lived in the central PRD region (GDstats, 2016) and two megacities, Guangzhou and Shenzhen, had over 13 and 11 million residents in 2015, respectively. There are over 20 ports located in the PRD region and eight of them surpassed 70 million tons of cargo throughput in 2015 (China Ports Year Book, 2016).

### 2.3. Air Quality Simulations

I used the regional chemical transport model Weather Research and Forecasting coupled with Chemistry (WRF-Chem) (Grell et al., 2005) version 3.5 for the ambient air quality estimation. The WRF-Chem simulated air quality within the three domain sizes, all centered at the PRD region (Figure 1). The largest model domain covers the half of Eastern China and neighboring South Asian Countries, with a  $27 \times 27$  km horizontal grid spacing. Two nested domains have finer resolutions of  $9 \times 9$  km and  $3 \times 3$  km, respectively. All three domains have 31 vertical levels, from the surface to 50 millibar (mb). The time period of the model simulation was July 2015, with five spin-up days from June 27<sup>th</sup> to June 30<sup>st</sup>. The model generated hourly concentrations for every simulation day. Further analyses, including model evaluation and monthly average concentrations of pollutants were based on the daily average concentrations from July 1<sup>st</sup> to July 31<sup>st</sup>.

I used the Regional Acid Deposition Model version 2 (RADM2) (Stockwell et al., 1990) for the gas-phase chemical mechanism, to predict the highly nonlinear O<sub>3</sub>, sulfate, nitric acid and hydrogen peroxide concentrations under various atmospheric conditions. For PM, I used the Modal Aerosol Dynamics Model for Europe with the Secondary Organic Aerosol Model (MADE/SORGAM) (Ackermann et al., 1998; Schell et al., 2001). MADE/SORGAM takes into account the aerosol dynamics, including formation (i.e. condensation, nucleation, coagulation), transport, dry deposition and aerosol-cloud interaction. MADE/SORGAM further predicts the mass of several particulate-phase species, including sulfate, ammonium, nitrate, sea salt, dust, BC, OC, and secondary organic aerosols (SOAs) in the three log-normal aerosol modes (Aitken, accumulation, and coarse).

Photolysis rates are obtained from the Fast-J photolysis scheme (Wild et al., 2000). I used the 6-h temporal resolution National Center for Environmental Prediction (NCEP) Global Forecast System gridded data as the model meteorological inputs. The simulated horizontal winds, temperature, and humidity were nudged to the respective meteorological fields. I also used initial and lateral boundary conditions from the global chemical transport model, the global Model for Ozone and Related Chemical Tracers (MOZART-4) (Emmons et al., 2010), to account for the initial and background chemical concentrations.

I used the Multi-resolution Emission Inventory of China (MEIC) (<http://www.meicmodel.org>) for the 2015 anthropogenic emissions in China, other than those from ships. For emissions for the rest of the regions in the domain out of China, I used the Regional Emission Inventory in ASia version 2 (REAS) (Kurokawa et al., 2013). Both MEIC and REAS inventories provide emissions of major primary and secondary air pollutant precursors, including NO<sub>x</sub>, SO<sub>2</sub>, VOCs, NH<sub>3</sub>, CO, and PM. PM in both inventories are classified into OC, BC, PM<sub>2.5</sub> and PM<sub>10</sub>. I used the Fire INventory from NCAR (FINN) for the year 2015 (Wiedinmyer et al., 2011) for biomass burning emissions and the Model of Emissions of Gases and Aerosols from Nature (MEGAN) version 2.1 (Guenther et al., 2012) for biogenic emissions based upon the weather and land use data. WRF-Chem calculated the dust and sea salt emissions online by using the dust transport model (Shaw et al., 2008) and sea salt schemes (Gong, 2003). Also added were the aircraft emissions of BC, CO, OC, PM<sub>2.5</sub>, NO<sub>x</sub>, and SO<sub>2</sub> from the Task Force Hemispheric Transport of Air Pollution (HTAP) emissions inventory (Janssens-Maenhout et al., 2015).

To evaluate a model's meteorological performance, I compared the simulated 2-meter temperature, wind speed, wind direction and relative humidity with the observed, taken from the National Oceanic and Atmospheric Administration (NOAA) National Climatic Data Center (NCDC) land-based stations (NCEI, 2017). Only four cities, Guangzhou, Shenzhen, Zhaoqing, and Hong Kong had data for 2015; thus, I chose the observed data from each city to evaluate the model results. I also evaluated the model performance of air pollutant concentration at nine government-controlled monitoring sites in the PRD region; each site represented a major city in the PRD region. Those cities were Guangzhou, Shenzhen, Zhuhai, Foshan, Zhongshan, Jiangmen, Dongguan, Huizhou, and Zhaoqing. The locations of both meteorological and air quality stations are shown in Figure 1. Based on the coordinates of these monitoring sites, I retrieved their located grids under the smallest domain ( $3 \times 3$  km) and compared the modeled results on the grid to the observed results.

The model performance was determined by statistical metrics including the correlation coefficient ( $r$ ), the normalized mean bias (NMB), the normalized mean error (NME), the mean fractional bias (MFB), the mean fractional error (MFE), and the root mean square error (RMSE) between the observed measures and modeled outputs (Chang and Hanna, 2004). The metrics are defined as:

$$r = \frac{\sum_{i=1}^n M_i O_i}{\sqrt{(\sum_{i=1}^n |M_i|^2)(\sum_{i=1}^n |O_i|^2)}} \quad [1]$$

$$NMB = \frac{\sum_{i=1}^n (M_i - O_i)}{\sum_{i=1}^n O_i} \times 100\% \quad [2]$$

$$NME = \frac{\sum_{i=1}^n |M_i - O_i|}{\sum_{i=1}^n O_i} \times 100\% \quad [3]$$

$$MFB = \frac{1}{N} \times \frac{\sum_{i=1}^n (M_i - O_i)}{\sum_{i=1}^n (M_i + O_i)/2} \times 100\% \quad [4]$$

$$MFE = \frac{1}{N} \times \frac{\sum_{i=1}^n |M_i - O_i|}{\sum_{i=1}^n (M_i + O_i)/2} \times 100\% \quad [5]$$

$$RMSE = \sqrt{\frac{\sum_{i=1}^n (M_i - O_i)^2}{n}} \quad [6]$$

Where  $i$  indicates each day,  $n$  indicates the total days during the simulation period,  $M$  indicates the modeled result and  $O$  indicates the observed measurement. I evaluated the model performance of  $PM_{2.5}$  based on the standards developed by Boylan and Russell (2006), which set the performance goals for  $PM_{2.5}$  at MFB less than or equal to  $\pm 30\%$  and MFE less than or equal to  $50\%$ . The performance criteria for  $PM_{2.5}$  were set at MFB less than or equal to  $\pm 60\%$  and MFE less than or equal to  $75\%$ . For  $O_3$ , both MFB and MFE were set at less than or equal to  $\pm 15\%$  and  $35\%$ , as recommended by Morris et al. (2005).

## 2.4. Ship Emissions

### 2.4.1 Ship Emissions for 2015

The 2015 ship emission inventories are derived from the International Council on Clean Transportation (ICCT) marine team by using their Systematic Assessment of Vessel Emission (SAVE) model. The ICCT's 2017 report (Naya et al., 2017) provides detailed methodology. The model systematically estimates ship emissions using the bottom-up method by coupling the

Automatic Identification System (AIS) data and the ship characteristic data (made available by IHS Fairplay). AIS data include the hourly location, speed, and draught for individual ships, and combined with ship-specific characteristics, the SAVE model estimates a ship's energy demand and emissions.

The SAVE model calculated the hourly emissions for each ship and then aggregated all ships within the domain to find the overall emissions at each hour, using the following equation:

$$E_{i,j} = \sum_{t=0}^{t=n} (P_{ME_i} \times LF_{i,t} \times EF_{ME_{i,k,l,m}} + D_{AE_{p,i,t}} \times EF_{AE_{j,k,l,m}} + D_{BO_{p,i,t}} \times EF_{BO_{j,m}}) \quad [7]$$

Where E is emissions (g/hour),  $P_{ME}$  is main engine power (kW), LF is main engine load factor (%),  $EF_{ME}$  indicates main engine emission factor (g/kWh),  $D_{AE}$  indicates auxiliary engine power demand (kW),  $EF_{AE}$  is auxiliary engine emission factor (g/kWh),  $D_{BO}$  indicates boiler power demand (kW) and  $EF_{BO}$  indicates boiler emission factor (g/kWh). i indicates each ship, j indicates each pollutant, k indicates engine type (main engines (MEs), auxiliary engines (AEs), or boilers (BO)), l indicates engine tier (Tier I, Tier II, Tier III), m indicates fuel type (residual oil, marine distillates oil (MDO), marine gas oil (MGO) or general diesel oil (GDO)), t indicates operating hour, and p indicates phases (cruise, maneuvering, anchor, or berth). I used BC, CO, PM, SO<sub>2</sub>, NO<sub>x</sub> and non-methane volatile organic compound (NMVOC) emissions estimates from the SAVE model as the air quality model input.

#### 2.4.2 Ship Emissions for 2030

The 2030 ship emissions are projected based on the 2015 gridded *baseline* emissions. I projected future ship emissions in 2030 under two scenarios: Business-as-usual (referred as *2030 BAU*) and with a PRD 200 nm ECA scenario (*2030 ECA*) (Figure 1 orange slash area). I decided on the

200 nm range based on the current North American ECA, which is within the 200 nm along the US east and west coasts. With this 200 nm range, all ships are required to comply with the ECA standards, which will be elaborated later in this section, while the BAU scenario does not require any ships to comply with them.

Two factors were considered to project the future ship emissions in 2030: fuel consumption and emission factors. The conceptual equation for projection is written as:

$$E_{2030} = (FC_{2015} \times SF_{2030\ FC}) \times (EF_{2015} \times SF_{2030\ EF}) \quad [8]$$

Where  $E_{2030}$  is the ship emissions in 2030 (g/hour),  $FC_{2015}$  is the fuel consumption in 2015 (g),  $SF_{2030\ FC}$  is the scale factor used to project the 2030 fuel consumption,  $EF_{2015}$  is the emission factor in 2015, and  $SF_{2030\ EF}$  is the scale factor used to project the 2030 emission factor. In short,  $SF_{2030\ FC}$  is based on the expected change of the future shipping demand and  $SF_{2030\ EF}$  is estimated due to the change of future emission control policies. The detailed methodology for both SFs is described next.

#### 2.4.2.1 Scale Factors (SFs) for Fuel Consumption

To estimate the SF for the 2030 fuel consumption ( $SF_{2030\ FC}$ ), I mainly considered three factors: future fleet turnover, future trade volume, and future Energy Efficiency Design Index (EEDI).

$SF_{2030\ FC}$  was calculated as:

$$SF_{2030\ FC} = \frac{[SF_{Power} \times SF_{Trade\ volume} \times SF_{EEDI}]}{SF_{dwt}} \quad [9]$$

Where  $SF_{Power}$  is the scale factor for engine power,  $SF_{Trade\ volume}$  is the scale factor for trade volume,  $SF_{EEDI}$  is the scale factor for EEDI and  $SF_{dwt}$  is the scale factor for deadweight tonnage.

A future fleet turnover model designed by ICCT provided  $SF_{Power}$  and  $SF_{dwt}$ . The model was built based on the following assumptions:

- The average lifetime for an oceangoing vessel is about 25 years;
- The total number of vessels in the world will not change;
- The average ship size will increase by 0.3-6% depending on ship classes;
- The average main engine power will increase by 2-8% depending on ship classes;
- The average deadweight tonnage will increase by 0.5-12% depending on ship classes;
- The overall fuel efficiency will increase as EEDI improves.

I estimated the future trade volume ( $SF_{\text{Trade volume}}$ ) based on historical data published by the United Nations Conference on Trade and Development (UNCTAD), which summarizes seaborne trade volume by region and by major cargo type annually. In this study, interpolating the historical data from 2006 to 2015 helped project the 2030 trade volume. Projections were based on the following assumptions:

- The world seaborne trade will continue growing because of increasing globalization and decreasing transportation cost.
- Asia will become the center of international trade.
- Containerized cargo and bulk cargo are still showing good momentum to grow, but likely with a less aggressive expansion rate.
- Liquefied Natural Gas (LNG) transport, however, will catch up in a fast pace, while crude oil trade will drag in the long term.

With the projected trade volume for 2030, I found the compound annualized growth rate (CAGR) as well as the overall growth rate over the 15-year period. The trade volume growth rates specific to cargo type can be uniquely tied to ship classes. For example, a class such as bulk carriers only carry major dry bulk cargo, like coal, grain, or ores, while oil tankers only carry crude oil and petroleum products. For ship classes whose corresponding cargo does not have specific forecast numbers, the overall trade growth rates for Asian developing countries were used instead.

The Energy Efficiency Design Index (EEDI), set forth by IMO, mandates that ships built after a certain date need to gradually become more energy efficient than the baseline fleet in terms of gCO<sub>2</sub>/ton-mile (MEPC.203(62), 2011). With the goal being to reduce greenhouse gas emissions from shipping, EEDI provides incentives for ships to become more efficient either by improving performance of the ship itself or by adopting optimized operations. In this study, I applied an average 20% improvement of EEDI in 2030 compared to 2015. Thus, the scale factor for EEDI (SF<sub>EEDI</sub>) is 80% in the above equation 9.

#### 2.4.2.2 Scale Factors (SFs) for Emission Factors

The SF<sub>EF</sub> (equation 8) for the future emission factors is determined by the associated policies and because ECA mainly targets a few pollutants, such as PM, SO<sub>2</sub> and NO<sub>x</sub>, the emission factors for those three pollutants will be primarily affected, while others such as CO and NMVOC will not.

The emission factor for SO<sub>2</sub> is determined by the sulfur content of fuels (Equation 10).

$$SO_x \left( \frac{g \text{ pollutant}}{g \text{ fuel}} \right) = 0.02 \times \text{Fuel sulfur content} \quad [10]$$

Current global average sulfur content for marine fuel is approximately 2.5% (Smith et al, 2015) and thus indicates that the current fuel sulfur content is 0.05 gSO<sub>2</sub>/g fuel.

Under the BAU scenario, I considered two policies: the IMO fuel sulfur cap and DECA 2.0. The IMO fuel sulfur cap starting in 2020 will require all IMO-regulated vessels to use fuel with less than 0.5% sulfur content globally. This cap would cause an 80% reduction in SO<sub>x</sub> emission factor, even under the BAU scenario, compared to current practices. DECA 2.0 refers to the upgraded DECA starting in 2019. Under the DECA 2.0 region, all ship fuels should be less than 0.5%, according to the current DECA (or DECA 1.0). In addition, all ships berthing in China or traveling within 12 nm coastline of Hainan Province will be required to use marine fuel with less

than 0.1% sulfur content. Thus, within the DECA 2.0 region, I will implement a 96% reduction in the SO<sub>x</sub> emission factor.

Under the ECA scenario, in addition to the policies that have already been mentioned for the BAU, a 200 nm ECA will be applied in the PRD coastline region. ECA enforces the 0.1% fuel sulfur content within the region; thus, a 96% reduction of the SO<sub>x</sub> emission factor would be applied to the whole region. The only difference between BAU and ECA scenarios, therefore, is an additional 200 nm ECA area that will use 0.1% sulfur content fuels.

PM emission factor is also related to the fuel sulfur content based on the *Third IMO Greenhouse Gas Study* (Smith et al., 2015). Thus, all aforementioned policies to reduce fuel sulfur content will have a positive spillover effect on PM as well. PM emission factor is also ship-specific because it is also due to the specific fuel oil consumption (SFOC) by ship classes and based on the usage of heavy fuel oil (HFO) or marine diesel oil (MDO) and marine gas oil (MGO), I applied different equations to calculate the emission factor (Smith et al., 2015):

$$PM_{HFO} \text{ (g pollutant)/(g fuel)}$$

$$= 1.35 + SFOC \times 7 \times 0.02247 \times (\% \text{ Fuel sulfur content} - 0.0246) \times SFOC$$

$$PM_{MDO/MGO} \text{ (g pollutant)/(g fuel)}$$

$$= 0.23 + SFOC \times 7 \times 0.02247 \times (\% \text{ Fuel sulfur content} - 0.0024) \times SFOC \quad [11]$$

On average, the IMO sulfur cap, which would be implemented globally in 2020, would result in a 50% reduction in PM emission factor and the ECA 0.1% fuel sulfur content would reduce PM emission factor by approximately 90%. The type of engine installed on ships determines the NO<sub>x</sub> emission factor. The IMO has assigned several tiers for marine diesel engines under MARPOL Annex VI (Table 2). Thus, the projection of the NO<sub>x</sub> emission factor considered the fleet's age

distribution in 2030. To project the 2030 NO<sub>x</sub> emission factor, it was assumed that all the new ships built after 2016 would follow the up-to-date Tier III. For the rest of the ships built before 2016, they would only meet Tier III within the ECA region. The current Tier III compliance technology is to install an aftertreatment device, such as Selective Catalytic Reduction (SCR), which could reduce NO<sub>x</sub> to harmless nitrogen gas (N<sub>2</sub>) when urea or ammonia is injected in the exhaust gas. After January 1, 2016, ships entering the North American ECAs must be Tier III compliant. The Baltic Sea and North Sea ECAs will also adopt the same Tier III standards for ships built after 2022. Ships are allowed to shut down their NO<sub>x</sub> aftertreatment while navigating in non-ECA regions. Under the BAU scenario, the study region will not require any ships to be Tier III compliant. Under the ECA scenario, it was assumed that the 200 nm ECA would enter into effect starting in 2025, meaning that only the Tier III compliant new ships built after 2025 can enter into the ECA region.

BC emission factors depend on the fuel type. ECA fuel sulfur regulations will be mostly achieved by switching to a cleaner fuel type. BC emission factors associated with different fuel types were taken from Comer et al. (2017). The emission factors for CO and NMVOC were unchanged from the 2015 emission factors. The SFs of emission factors for all pollutants are summarized in Table 3.

## **2.5. Emission Scenarios**

I created four scenarios for ship emissions (Table 1). All scenarios used the exact same land source emissions from the MEIC and REAS inventories. Each scenario, however, had different ship emissions. The *Baseline* Scenario excluded all ship emissions and only contained all other land source emissions in 2015. The *2015 With Ship* Scenario added the 2015 ship emissions to

the *Baseline*. The *2030 BAU* Scenario added *2030 BAU* ship emissions to the *Baseline*. The *2030 ECA* Scenario added the 2030 projected ship emissions with the implementation of ECA to the *Baseline*.

To find the upper bound impacts on air quality from ship emissions, I modeled the month of July, which is the monsoon season and when southeastern winds transport ship emissions from the sea to the land (Lu et al., 2009). During this season, impacts from ship emissions towards the PRD cities most likely reach maximum. Some studies have also shown that July has the highest contributions of ship emissions towards land (Chen et al., 2018; Liu et al., 2018).

## 2.6. Ship Impacts

I quantified the ambient air quality impacts due to ship emissions in 2015 as the increased concentrations by adding ship emissions to the *Baseline*, as follows:

$$\Delta C_{SHIP-RELATED} = C_{With Ship} - C_{Baseline} \quad [12]$$

Where  $\Delta C_{SHIP-RELATED}$  represents the increased concentrations due to the addition of ship emissions and  $C_{With Ship}$  and  $C_{Baseline}$  indicate the concentrations for the *2015 With Ship* Scenario and for *Baseline*, respectively. The contributions of ship emissions to the ambient air concentrations were calculated as,

$$\text{Ship Contribution\%} = \frac{\Delta C_{SHIP-RELATED}}{C_{2015 With Ship}} \quad [13]$$

To estimate the improved air quality brought by ECA, I compared the pollutant concentrations from the model results in *2030 BAU* Scenario and *2030 ECA* Scenario. I calculated the ECA impacts as the decreased concentrations due to ECA implementation as:

$$\Delta C_{ECA} = C_{2030\ BAU} - C_{2030\ ECA} \quad [14]$$

Where  $\Delta C_{ECA}$  is the decreased concentrations due to ECA implementation,  $C_{2030\ BAU}$  indicates the concentrations for the *2030 BAU* scenario, and  $C_{2030\ ECA}$  indicates the *2030 ECA* scenario.

## 2.7. Health Impact Estimation

The health impacts due to ship-caused  $PM_{2.5}$  and  $O_3$  increases were estimated for both acute (short-term) and chronic (long-term) mortalities. For the acute mortality, I calculated the total number of deaths in all-cause, cardiovascular disease (CVD), and respiratory mortalities for both  $PM_{2.5}$  and  $O_3$ . The relative risk (RR) due to pollution for each health endpoints was derived from the pooled estimate of the increased mortality due to  $10\ \mu g/m^3$  increase of  $PM_{2.5}$  or  $O_3$  concentrations from the PRD-specific epidemiological time-series studies by Lin et al (2016) and Tao et al (2012).

The long-term integrated exposure response (IER) function for each health point is developed by Burnett et al. (2014), which is widely used to estimate the global burden of disease attributable to  $PM_{2.5}$  exposure over the entire global exposure range. The IER model is written as:

$$RR(z) = \begin{cases} 1, & z < z_{cf} \\ 1 + \alpha \{1 - e^{[-\gamma(z-z_{cf})]^\delta}\}, & z \geq z_{cf} \end{cases} \quad [15]$$

Where  $z$  is the exposure to  $PM_{2.5}$  in  $\mu g/m^3$  and  $z_{cf}$  is the counterfactual concentration, below which no additional risk is assumed. The parameters (i.e.  $\alpha$ ,  $\gamma$  and  $\delta$ ) for each health endpoint are decided by fitting a curve to RR data taken from studies on ambient air pollution, secondhand tobacco smoke, household solid cooking fuel, and active smoking. Since there are only few cohort studies performed in China, and none of them has been further validated, the IER functions are currently regarded as the best estimate of the long-term mortality in China. The

IER functions are developed for causes of mortality including ischemic heart disease (IHD), cerebrovascular disease (CEV), chronic obstructive pulmonary disease (COPD), and lung cancer (LC). For the chronic O<sub>3</sub> exposures, since there is no comprehensive IER studies like PM<sub>2.5</sub>, I simply adopted RRs from a cohort study by Jerrett et al. (2009), the RRs for CVD, respiratory, IHD, etc. However, significant uncertainty might remain in the O<sub>3</sub> chronic mortality.

Both acute and chronic mortalities were estimated by a log-linear model [Equation 17] which links the air pollution concentration difference and health endpoints, using the concentration-response function (CRF) coefficients derived from the RR from Equation [16],

$$\beta = \frac{\ln(RR)}{\Delta c} \quad [16]$$

$$\Delta y = y_0 \{1 - e^{-\beta(C_1 - C_0)}\} \times \text{Pop} \quad [17]$$

Where RR is the relative risk,  $\beta$  is the coefficients of exposure-response functions,  $\Delta c$  is the unit of increased air pollution concentrations (10  $\mu\text{g}/\text{m}^3$  or 10 ppb in most time-series studies),  $\Delta y$  is the increased incidence due to ship emissions in 2015 or the decreased incidence due to ECA implementation in 2030,  $y_0$  is the base incidence rate, and  $C_1 - C_0$  is the increased air pollutant concentrations due to ship emissions in 2015 or the decreased concentrations due to ECA implementation in 2030.

I extracted the monthly average PM<sub>2.5</sub> and monthly average 8-hour maximum O<sub>3</sub> from the smallest domain in the model (3 × 3 km) as the input air pollutant concentrations ( $C_0$  and  $C_1$ ). The Gridded Population of the World (GPW) fourth version (v4) provides the 2015 population gridded data (1 × 1 km) (NASA, SEDAC) and the grid cells were aggregated to match with the air pollution grid cells. I obtained the population projections for 2030 from the United Nations

Economic and Social Commission for Asia and the Pacific (UN ESCAP) Probabilistic Population Projections. Based on the estimation from the UN Department of Economic and Social Affairs (DESA) in their 2017 revision, the median population projection for mainland China (excluding Macao, Hong Kong, and Taiwan) for 2030 is 1.44 billion, compared to 1.40 billion in 2015. Since no gridded 2030 population data are available, I used the gridded 2015 population, combined with the ratio of the total population in 2030 to the base year 2015 for each  $3 \text{ km} \times 3 \text{ km}$  grid.

I obtained the baseline incidence of all-cause, CVD, and respiratory diseases for the six main cities in PRD from the Guangdong Provincial Center for Disease Control and Prevention (Lin et al., 2016). Due to a lack of city-specific baseline incidence rates for the rest of the diseases, I applied the provincial baseline incidence rate in 2015 (Personal communication, Peng Yin and Health Effects Institute), to all cities in Guangdong Province. All the death incidences were estimated in each  $3 \text{ km} \times 3 \text{ km}$  grid and then aggregated within each city or the whole Guangdong province.

## **2.8 Technical Support**

I used R (R core team, 2013) and Python (Rossum, 1995) for data analysis and figure preparation, ArcGIS (ESRI, 2012) and QGIS (QGIS Development Team, 2009) for geospatial analysis and visualization, and Fortran (Ortega, 1994) for WRF-Chem. Lastly, I used IDL (Research Systems, Inc. 1995) and NCL (The NCAR Command Language, 2017) for the processing of model input and output.

## **3. Results**

### 3.1 Emissions

Table 5 describes the emissions of PM<sub>2.5</sub>, SO<sub>2</sub> and NO<sub>x</sub> for all the four scenarios. In 2015, there were 9,237 kt/year of PM<sub>2.5</sub>, 18,353 kt/year of SO<sub>2</sub> and 25,701 kt/year of NO<sub>x</sub> emitted in China from all the major land sources (i.e. power plant, residential, land transportation, agriculture, and industry), except shipping. In the PRD region for shipping, 158 kt/year of PM<sub>2.5</sub>, 350 kt/year of SO<sub>2</sub> and 669 kt/year of NO<sub>x</sub> were emitted in the same year and they accounted for about 1.7%, 1.9% and 2.6% of total emissions in China.

Ship emissions have varied greatly among the three scenarios. Table 5 also summarizes the difference between ship emissions within the ECA 200 nm region. In 2015, within the 200 nm ECA region, I estimated 11.3 kt/year of PM<sub>2.5</sub>, 89.5 kt/year of SO<sub>2</sub> and 141.9 kt/year of NO<sub>x</sub> by ships. Ship-emitted PM<sub>2.5</sub>, SO<sub>2</sub> and NO<sub>x</sub> accounted for 7%, 20%, and 17% of all emissions in the entire PRD area (PRD + 200 nm ECA). Figure 2 compares the monthly mean surface emissions of five major pollutants (PM<sub>2.5</sub>, EC, CO, NO<sub>x</sub>, and SO<sub>2</sub>) in July 2015 for the two scenarios:

*Baseline* and *2015 With Ship* emissions. I found that there were more emissions in the central PRD area, including Guangzhou, Shenzhen, Zhuhai, Dongguan and Hong Kong, compared to the further inland cities. Ships emitted negligible amount of EC, CO and PM<sub>2.5</sub>, but significant amounts of SO<sub>2</sub> and NO<sub>x</sub>.

For the *2030 BAU* scenario, I estimated 9.9 kt/year of PM<sub>2.5</sub>, 27.0 kt/year of SO<sub>2</sub> and 197.9 kt/year of NO<sub>x</sub> emissions from ships within the 200 nm ECA region. Compared to the 2015 ship emissions, this is a 12% and 70% decrease for PM<sub>2.5</sub> and SO<sub>2</sub>, but a 39% increase in NO<sub>x</sub>. Under the *2030 ECA* scenario, I estimated that 4.3 kt/year of PM<sub>2.5</sub>, 6.4 kt/year of SO<sub>2</sub>, and 172.3 kt/year of NO<sub>x</sub> would be emitted from ships within the 200 nm ECA region, resulting in a 57%,

76% and 13% decrease of PM<sub>2.5</sub>, SO<sub>2</sub>, and NO<sub>x</sub>, respectively, from the 2030 BAU scenario.

Comparing ship emissions between 2030 ECA and 2015 With Ship scenarios, I found that the PM<sub>2.5</sub> and SO<sub>2</sub> under 2030 ECA would decrease by 62% and 93% respectively, but NO<sub>x</sub> would increase by 21%. The cause of these differences will be elaborated in the discussion section.

Figure 3 illustrates the gridded ship emissions of PM<sub>2.5</sub>, SO<sub>2</sub>, and NO<sub>x</sub> in July for the three scenarios with ship emissions (2015 With Ship, 2030 BAU, and 2030 ECA). All three pollutants show that the most heavily trafficked route is along the coast, especially on the eastern side of the PRD region.

### 3.2 Model Evaluation

Table 6 summarizes the model performance related to meteorological parameters. The 2-meter temperature at Guangzhou between the simulated and observed had a correlation of 0.9 and an NMB of 0.3%. Small NMB values were also found at Shenzhen (0.2%) and at Zhaoqing (-0.3%), as well as in Hong Kong (-0.03%). The correlation coefficients between the observed and simulated for the 2-meter temperature in the sites of Shenzhen, Zhaoqing and Hong Kong were 0.8, 0.7, and 0.8, respectively. The model slightly underestimated the relative humidity among all the four sites, and the correlation between the observed and the simulated were 0.50, 0.60, 0.52, and 0.65 and NMB of -16%, -12%, -1.6% and -2.6%.

The model also underestimated the wind speed in Guangzhou, Shenzhen and Hong Kong, with a correlation between the modeled and observed being 0.85, 0.80, and 0.83 and NMB of -15%, -36%, and -36%. The model, however, overestimated the wind speed at Zhaoqing, with a correlation of 0.5 and NMB of 32%. Figure 4 shows the comparison between the observed and modeled wind. The direction of each widget represents wind direction and the color represents

wind speed: the darker the color, the faster the wind. The length of each widget shows the number of hours that were observed or modeled within that direction where the wind comes from. I found that the southerly wind was the most dominant, indicating that wind most often blew from the ocean to the land. This result reconfirmed that the impact of ship emissions will be the largest in July due to the dominant wind direction from the ocean to land.

Figure 5 and 6 present the comparison of modeled and observed PM<sub>2.5</sub> and O<sub>3</sub> concentrations and the comparison of modeled and observed SO<sub>2</sub> and NO<sub>2</sub> concentrations, respectively. I evaluated these four pollutants, since PM<sub>2.5</sub> and O<sub>3</sub> are the major pollutants causing health impacts, and SO<sub>2</sub> and NO<sub>x</sub> are the two major pollutants emitted by ships. Table 7 describes the statistical results for these four pollutants.

I found that the model overestimated the PM<sub>2.5</sub> concentrations in some cities, including Guangzhou and Shenzhen. This might be due to an underestimated wind speed and precipitation. As I mentioned earlier, I found that the modeled wind speed is smaller than the observed, which could predict more stagnant air in some cities. Nevertheless, the PM<sub>2.5</sub> model performance for all cities still met the goal (MFB  $\leq \pm 30\%$  and MFE  $\leq 50\%$ ), suggested by Boylan and Russell (2006).

### **3.3. Air Quality Impacts**

#### **3.3.1 Year 2015**

Tables 8 and 9 summarize the comparison of the PM<sub>2.5</sub> and O<sub>3</sub> concentrations under the *Baseline* and *2015 with ship* emissions scenarios, respectively. For the *Baseline* and *2015 With Ship* scenarios, the monthly mean concentrations of PM<sub>2.5</sub> from model were 31.3 and 32.4  $\mu\text{g}/\text{m}^3$  over

Guangdong province, respectively. Shenzhen was the individual city most impacted, with a  $4.0 \mu\text{g}/\text{m}^3$  increase in  $\text{PM}_{2.5}$  concentrations due to ship emissions. I found that Shanwei, Foshan, Huizhou, and Guangzhou all had over  $2.0 \mu\text{g}/\text{m}^3$  increase in  $\text{PM}_{2.5}$  concentrations due to ship emissions. For  $\text{O}_3$ , the monthly average 8-hour maximum concentrations for the PRD region were 49.0 and 50.6 ppb, for the baseline and *2015 With Ship* scenarios, respectively. The most impacted city was Shanwei, with a 5.79 ppb increase in  $\text{O}_3$ . Zhuhai, Shenzhen, and Huizhou were also greatly impacted by more than a 2.0 ppb increase of  $\text{O}_3$ .

Figure 7 presents the monthly average concentrations for the *Baseline* and *2015 With Ship* scenarios, the increased concentrations due to ships in 2015, and the percentage of ship-related concentrations to the all-source concentrations for four major pollutants (i.e.  $\text{O}_3$ ,  $\text{PM}_{2.5}$ ,  $\text{SO}_2$ , and  $\text{NO}_x$ ) within the finest resolution domain. For  $\text{O}_3$ , I found that the most affected area was the southeast of the PRD and the greatest increase (over 6 ppb increase) occurred above the sea. For  $\text{PM}_{2.5}$ , the greatest impact due to ship emissions also took place in the southeast region which is primarily ocean. The two short-lived pollutants,  $\text{SO}_2$  and  $\text{NO}_x$ , increased by  $10 \mu\text{g}/\text{m}^3$  in the northern and eastern areas of the PRD, where Guangzhou, Shenzhen, and Hong Kong were all located.

Interestingly, I observed a tiny area where the  $\text{PM}_{2.5}$  concentrations actually decreased after adding ship emissions. The reason might be that the addition of ship emissions changed the WRF meteorological fields slightly, including the wind pattern, cloud formation, precipitation, etc. Figure 8 shows that the wind pattern and temperature have indeed been altered after adding the ship emissions. Those areas where I found decreased concentrations also had an increase in wind

speed that diffused the pollution more rapidly, and thus explaining the decrease in concentrations after the ship emissions were added.

### **3.3.2. Year 2030**

The pollutant concentration differences between the *2030 BAU* and *2030 ECA* scenarios are shown in Figure 9. These differences represent the potential air quality improvement that ECA could provide to the PRD cities. Figure 9 illustrates four major pollutants, PM<sub>2.5</sub>, O<sub>3</sub>, SO<sub>x</sub> and NO<sub>x</sub>, and their concentrations would be reduced in most of the PRD region under *2030 ECA* scenario, although some areas would not have a significant decrease. The monthly average PM<sub>2.5</sub> concentrations in the PRD region are 31.5 µg/m<sup>3</sup> and 30.7 µg/m<sup>3</sup> for the *2030 BAU* and the *2030 ECA* scenarios. Hong Kong and Shenzhen would benefit the most if ECA was implemented, as their monthly average PM<sub>2.5</sub> is projected to decrease by 1.9 and 1.3 µg/m<sup>3</sup>, respectively.

The monthly average O<sub>3</sub> concentration in *2030 BAU* for the PRD region was 42.3 ppb and was fairly similar to that of the ECA scenario (42.0 ppb). I found that Shenzhen and Dongguan would benefit the most from ECA but the O<sub>3</sub> decreases in both cities were only 0.47 and 0.40 ppb, respectively. NO<sub>x</sub> and SO<sub>2</sub> concentrations also decreased the most (over 2 µg/m<sup>3</sup>) in the Eastern PRD, where Shenzhen, Dongguan, and Hong Kong are located.

## **3.4. Health Impacts**

### **3.4.1. Premature mortality associated with acute air pollution exposures in 2015**

In 2015, I found that PM<sub>2.5</sub> concentrations due to ship emissions caused an estimated 155 (95% CI: 130, 181) acute premature deaths in six major cities in the Guangdong Province (excluding Hong Kong), which included Guangzhou, Shenzhen, Jiangmen, Foshan, Dongguan, and Zhuhai.

Acute premature deaths due to the exposure to O<sub>3</sub> concentrations from ship emissions were predicted to be 115 (95% CI: 89, 142) (Figure 10). Among the PM<sub>2.5</sub>-related deaths, CVD deaths accounted for 54% of total deaths (84 cases, 95% CI: 69, 99) and respiratory mortality accounted for about 13% of total deaths (20 cases, 95% CI: 12, 28). On the other hand, the ship-associated O<sub>3</sub> increase predicted 64 (95% CI: 45, 83) excess CVD deaths and 24 (95% CI: 16, 31) excess respiratory deaths. Acute mortality predictions are summarized in Table S1.

Among the six cities, Guangzhou had the largest number of total predicted excess acute deaths (104 incidences, 95% CI: 76, 112). The biggest reason is that Guangzhou has the largest population of about 14.7 million people in 2015, compared to the second largest city of Shenzhen, with population of 12.9 million. Jiangmen had the second most predicted excess deaths [55 with 95% CI: 45, 66] in 2015 due to its highest baseline incidence rate for each health endpoint among all six cities. Shenzhen also had 51 (95% CI: 42, 62) predicted excess deaths which are also due to its second largest population and a substantial concentration increase due to ship emissions. The other three cities, Dongguan, Zhuhai and Foshan, shared nearly a quarter of predicted excess deaths among the six cities.

### **3.4.2. Premature mortality associated with chronic air pollution exposures in 2015**

Ship-related chronic exposure to PM<sub>2.5</sub> resulted in a total of 2,349 (95% CI: 989, 3345) predicted excess premature deaths in the PRD region due to IHD, COPD, LC, CEV, and respiratory infection combined (Figure 11). I found the largest number of predicted excess premature deaths in Shenzhen (651 cases, 95% CI: 292, 868) for all-cause mortality, among the twenty cities. The reason that most predicted excess deaths were found in Shenzhen is due to its dense population and substantial contribution of ship emissions. There were also large numbers of predicted

premature deaths in Hong Kong (370, 95% CI: 116, 608) and Guangzhou (346, 95% CI: 155, 462), since both are also highly populated cities. More than a hundred incidences of predicted excess premature mortality were also found in Foshan, Jiangmen, Dongguan, Huizhou and Shanwei due to ship emissions in 2015.

Ship-related chronic exposure to O<sub>3</sub> concentrations resulted in a total of 994 (95% CI: 223, 1534) predicted excess premature deaths in the PRD region due to CVD and respiratory deaths combined (Figure 12). Among CVD death incidences (791 cases, 95% CI: 171, 1292), approximately 48% (378, 95% CI: 78, 650) died from IHD. The lower-respiratory disease contributed to fewer predicted deaths than CVD as I predicted 203 (95% CI: 52, 243) excess deaths from the respiratory disease. Similar to PM<sub>2.5</sub>, the increased O<sub>3</sub> also caused three mega cities, Guangzhou, Shenzhen, and Hong Kong to have the highest predicted chronic mortality from CVD and respiratory infection. Outside of those three mega cities, I also predicted more than fifty excess deaths due to ship-induced chronic O<sub>3</sub> exposure in Dongguan, Huizhou, and Shanwei.

### **3.4.3 Premature mortality associated with chronic air pollution exposures in 2030**

For future scenarios, only chronic mortality was predicted due the lack of baseline incidence data. I predicted 2,545 (95% CI: 1,077, 4,481) ship-related chronic excess deaths under *2030 BAU*, where 1,525 (95% CI: 616, 2,377) of these were due to ship-related PM<sub>2.5</sub>. Compared to 2015, the PM<sub>2.5</sub>-related deaths reduced by 35%. On the contrary, premature deaths due to O<sub>3</sub> exposure in 2030 were greater than in 2015. In 2030, O<sub>3</sub>-related mortality reached 1,020 deaths compared to 994 in 2015, resulting in a 2.6% increase.

### 3.4.4 Avoided mortality due to ECA implementation

The potential health benefits provided by ECA in 2030 were predicted by comparing PM<sub>2.5</sub> and O<sub>3</sub> concentrations with and without ECA implementation. I found that by implementing ECA, 1,044 and 143 excess deaths could be avoided by a decreased PM<sub>2.5</sub> and O<sub>3</sub>, respectively. These values are equivalent to 68% and 14% of all-cause deaths in 2030 BAU scenario, due to PM<sub>2.5</sub> and O<sub>3</sub> exposure. Combining the total mortality from two pollutants, 47% of deaths could be avoided by ECA compared to the BAU scenario. The detailed excess death incidence numbers for each health endpoint are given in Table 10.

## 4. Discussion

In 2015, ship emissions were a major pollution source in the PRD region, accounting for 7%, 20%, and 17% of PM<sub>2.5</sub>, SO<sub>2</sub> and NO<sub>x</sub> among all emitting sources, respectively. Ship emissions decreased significantly for both PM<sub>2.5</sub> and SO<sub>2</sub> in 2030 from the 2015 baseline levels, even under 2030 BAU. There are two main reasons for the decrease. First, ships in 2015 were still using the 2.5% sulfur content fuels. However, DECA was implemented in October 2016 in the coastal PRD region for ships at berth and will apply to all ships entering the area by 2019. In 2030, I therefore assumed the sulfur content of the fuel would be 0.5% within the DECA area. Second, starting in 2020, the IMO requested all oceangoing ships comply with 0.5% sulfur content limit in the global domain, which will further decrease the SO<sub>2</sub> emissions from ships worldwide.

Therefore, based on these two reasons, I assumed SO<sub>x</sub> emissions would considerably decrease in 2030 regardless of ECA. The amount of primary PM emissions from ships is a direct result of the reduced sulfur content in the fuels, since the PM emission factor is well related to the sulfur content in the fuels, as I discussed in the emission projection methodology for Equation [11]. In

addition, fewer secondary inorganic aerosols will be formed as SO<sub>2</sub> emissions decrease, further lowering the PM concentration in the ambient air.

On the contrary, NO<sub>x</sub> emissions from ships increased by 50 kt/year from 2015 to the *2030 BAU* scenario because there has been a lack of strong global policy for NO<sub>x</sub> control. The current global NO<sub>x</sub> emission control, MARPOL Annex VI NO<sub>x</sub> Tier II emission standards, was adopted in 2011. The NO<sub>x</sub> Tier III emission standards only target ships built after 2016 and only when they travel inside the North American ECAs. In China, the current DECA does not require newer ship engines to be Tier III compliant for new ships. Thus, under the *2030 BAU* scenario, I assumed no further policies, resulting in the *2030 BAU* and *2015 With Ship* scenarios having the same NO<sub>x</sub> emission standards. As tonnage demand is expected to increase annually, the additional ships in the *2030 BAU* scenario led to higher NO<sub>x</sub> emissions compared to the *2015 With Ship* scenario.

Under the *2030 ECA* Scenario, I found a significant reduction in ship emissions of 57% and 76% for PM<sub>2.5</sub> and SO<sub>2</sub> respectively, and a moderate emission reduction (13%) for NO<sub>x</sub>, compared to the *2030 BAU*. PM<sub>2.5</sub> and SO<sub>2</sub> emissions reductions are due to the drop in the sulfur content in fuels from 0.5 to 0.1% inside of the ECA region. NO<sub>x</sub> emissions showed a 13% decrease compared to the BAU scenario after adopting the ECA NO<sub>x</sub> Tier III emission standards for the newly constructed ships within ECA when I projected the *2030 ECA* scenario emissions. In contrast, I expected all ships to have the Tier II engine standards under the *2030 BAU* scenario. Compared to Tier II, the NO<sub>x</sub> Tier III emission standards are much more stringent, as mentioned earlier. Since I assumed that ECA would be established in 2025, all new ships built between 2025 and 2030 followed the NO<sub>x</sub> Tier III emission standards. Because ships built before 2025

would be grandfathered to update to Tier III, so the NO<sub>x</sub> emission reduction benefit was rather limited. As a result, ECA would then lead to a moderate decrease in NO<sub>x</sub> in 2030 compared to the BAU scenario. However, if the ECA could have been implemented earlier than 2025, the NO<sub>x</sub> emission control would be more beneficial as more ships would need to follow the more stringent Tier III emission standards earlier.

I found that ship emissions caused an increase in pollutant concentration in the PRD region and the most affected area due to ship emissions was the southeast. In 2015, an average increase of 1.1 µg/m<sup>3</sup> increase for PM<sub>2.5</sub> concentrations and 1.62 ppb for O<sub>3</sub> concentrations increase were found in PRD and the southeast region. Cities such as Shenzhen, Dongguan, Huizhou, Shanwei and Hong Kong observed over a 2 µg/m<sup>3</sup> increase of PM<sub>2.5</sub> and a 2 ppb increase of O<sub>3</sub>. The incremental PM<sub>2.5</sub> and O<sub>3</sub> caused 155 and 115 death incidences due to acute exposure, and 2,349 and 994 death incidences due to chronic exposure. I found that ship-related mortality accounts for 1.3% of total cerebrovascular disease (CEV), 0.8% of chronic obstructive pulmonary disease (COPD), 0.8% of ischemic heart disease (IHD), 0.4% of lower respiratory infections, and 0.2% of lung cancer (LC) in Guangdong Province.

In 2030, I roughly predicted baseline mortality under the *2030 BAU* scenario and then assessed the potential health benefits due to ECA implementation. Although there is a large uncertainty associated with the mortality prediction for 2030, my results found that the potential health benefits from ECA could be substantial as I expect that 68% of deaths due to PM<sub>2.5</sub> and 14% of deaths due to O<sub>3</sub> could be avoided. Overall, ECA could prevent 47% of total deaths due to the exposure to PM<sub>2.5</sub> and O<sub>3</sub>. These mortality reduction ratios are also surprisingly similar to the ship emission reduction rates of 76% of SO<sub>2</sub>, 56% of the primary PM<sub>2.5</sub> and 13% of NO<sub>x</sub>

reduction from the BAU scenario. Thus, I infer that the percentage of mortality reduction is equivalent to that of emission reduction. It delivers the key message to the Chinese government that the strength of ship emission reduction directly determines the health benefit feedbacks.

I compared my results with two previous studies. Liu et al. (2016) have found that 18,000 premature deaths were expected in 2013 in the mainland China. According to the premature deaths I expected (3,613 deaths from both acute and chronic exposure), the PRD cities accounted for 20% of deaths in China due to ship emissions in the Chinese coast. Winebrake et al. (2009) have compared the global shipping mortality in 2012 under global 0.5% and coastal 0.1% sulfur limit scenarios. Their scenario setup is similar to the *2030 BAU* and *2030 ECA* scenarios in this thesis. They expected that approximately 15,000 premature deaths due to lung cancer and CVD could be avoided by adopting the ECA sulfur standard in every coastal region in the world. I found that 564 premature deaths could be avoided from those two diseases in the PRD region under the ECA scenario. This indicates that 3.8% of the avoided mortality from ECA in the world would be from the PRD region.

The study could be improved in several ways. First, I only simulated air quality for one month and then applied the monthly results to estimate annual average concentrations in 2015 to identify health effects due to ship emissions and ECA implementation. The number of deaths might be overestimated, as our simulation period is chosen to be when the effect from ship emissions on land are the greatest based on the previous studies (Chen et al., 2018; Liu et al., 2018). However, the number of deaths might also be underestimated because winter in the PRD has a higher PM<sub>2.5</sub> concentration in general, and the ship increased concentrations could be more noteworthy when simulating the model. Therefore, the final outcomes remain uncertain when

only modeled for one month and I might want to model multiple months in the future studies. Moreover, the choice of the year could also impact the study results. I chose the year of 2015 due to the data availability of both anthropogenic emissions and ship emissions. The precipitation in 2015 summer is the highest among the year periods from 2011 to 2017 (WorldWeatherOnline, 2018). If I chose a low-precipitation year instead, the  $PM_{2.5}$  concentrations would have been higher because of less wet scavenging.

Second, the model has not perfectly forecasted the observed results, as mentioned in the model evaluation section. It might be due to following reasons. First, on average, the modeled wind had a smaller wind speed than the observed wind. The modeled  $PM_{2.5}$  was also overestimated because a smaller wind speed could cause less aerosols to be transported and therefore the polluted air being stagnant in the research domain. In addition, due to the uncertainty of the emission inventory itself, the model might output a higher concentration than the observed due to the excess emission. As a result, the model has overestimated the  $PM_{2.5}$  concentration and this might further link to a higher premature mortality when estimating the health impact.

Third, according to the IER function that I used to estimate the chronic mortality, higher ambient pollution concentration results in a lower relative risk; As the model overestimated the pollutant concentrations in some cities, I could have underestimated the mortality in these cities when modeled concentrations are higher than observed concentrations. Third, due to data availability, I ran the model using 2015 land emissions for the two 2030 scenarios. That is the reason why I did not analyze absolute concentrations and focused only on the relative concentrations for our health benefit prediction for 2030.

There is also a high level of uncertainty in my estimates due to the following reasons. First, the population data derived from UN DESA have eight scenarios under different fertility and mortality patterns. The gridded population in 2030, however, simply escalated the 2015 gridded population by a scale factor, without considering any future migrations among cities. Similar uncertainty also exists in the baseline incidence rate in 2030. Furthermore, I used the same relative risk to estimate the health benefits in 2030, which could also cause an overestimation. The medical science is advancing rapidly, so the actual relative risk in 2030 might be much lower than in 2015.

One more source of uncertainty originated from the chronic mortality model IER itself, which was built based on many strong assumptions. The model has to be further improved to estimate the mortality more accurately. In fact, the recent studies have been done to develop alternative models other than the IER model. For example, Burnett et al. (2018) introduced a new model called the Global Exposure Mortality Model (GEMM), which relaxes the contentious assumptions in the IER and builds the hazard ratio function based only on cohort studies of outdoor air pollution. According to that study, they argue that the GEMM model would predict much larger health benefits by reducing  $PM_{2.5}$  than the previous IER model. Further research and the validation of GEMM is required.

Expected health benefits from ECA are obvious, as I quantified a 48% reduction in deaths due to  $PM_{2.5}$  exposure to the BAU scenario. However, to ultimately determine the net benefits from ECA, I should also perform a cost-effective analysis to estimate the increasing costs for the stakeholders when ECA is being implemented. Another ongoing study by ICCT will focus on the

costs for ship owners and shipping companies to comply with the ECA standard. Based on these estimates, I can combine both costs and benefits and estimate the net benefits of ECA. In addition, the ECA application is a long-lasting process, which usually takes more than five years from the initial application to the final implementation. Thus, it might be difficult to see a Chinese ECA fully implemented by 2030, when it is only established in 2025, as I assumed in this study. Moreover, the actual ECA range could be much smaller than 200 nm. I chose this value because that is the greatest range currently adopted in the world, as found in the North American ECAs. The current DECAs in China indeed only have a 12 nm range. Undeniably, the health benefits will be lower if the ECA range was smaller than 200 nm. Further studies are essential to strengthen the ECA benefits and to facilitate a larger ECA to be implemented at an earlier period.

## **5. Conclusion**

This study used WRF-Chem to estimate the contribution that ship emissions make to the ambient air quality in the PRD region and used concentration-response function to estimate impacts on ship-caused mortality. In 2015, ship emissions resulted in 1.1  $\mu\text{g}/\text{m}^3$   $\text{PM}_{2.5}$  and 1.62 ppb  $\text{O}_3$  increases within Guangdong Province and over 3,300 excess death in 2015 due to ship-related  $\text{PM}_{2.5}$  and  $\text{O}_3$  concentration increases.

Based on the potential health benefits for ECA in the PRD region. I predicted that ECA could decrease  $\text{PM}_{2.5}$  (0.83  $\mu\text{g}/\text{m}^3$ ) and  $\text{O}_3$  (0.37 ppb) from the business as usual (BAU) scenario in 2030. ECA implementation could avoid 1,044 and 143 excess deaths by the reduced concentrations of  $\text{PM}_{2.5}$  and  $\text{O}_3$ , compared to the BAU scenario. The premature mortality reduction ratios for  $\text{PM}_{2.5}$  and  $\text{O}_3$  are 68% and 14%, with an overall reduction of 47% for both

pollutants. Although my results contain large uncertainty, the health impacts due to ship emissions are non-negligible and an ECA establishment in the PRD region could notably reduce mortality.

## 6. References

- Ackermann, I. J., Hass, H., Memmesheimer, M., Ebel, A., Binkowski, F. S., and Shankar, U.: Modal aerosol dynamics model for Europe: development and first applications, *Atmos. Environ.*, 32, 2981–2999, doi:10.1016/S1352-2310(98)00006-5, 1998
- Boylan, J. W. and Russell, A. G.: PM and light extinction model performance metrics, goals, and criteria for three-dimensional air quality models, *Atmos. Environ.*, 40, 4946–4959, doi: 10.1016/j.atmosenv.2005.09.087, 2006.
- Burnett, R., Chen, H., Szyszkowicz, M., Fann, N., Hubbell, B., Pope, C. A., ... Spadaro, J. V. (2018). Global estimates of mortality associated with long-term exposure to outdoor fine particulate matter. *Proceedings of the National Academy of Sciences*, 201803222. <https://doi.org/10.1073/pnas.1803222115>
- Burnett Richard T., Pope C. Arden, Ezzati Majid, Olives Casey, Lim Stephen S., Mehta Sumi, ... Cohen Aaron. (2014). An Integrated Risk Function for Estimating the Global Burden of Disease Attributable to Ambient Fine Particulate Matter Exposure. *Environmental Health Perspectives*, 122(4), 397–403. <https://doi.org/10.1289/ehp.1307049>
- California Air Resources Board (CARB), 2014. Shore Power for Ocean-Going Vessels. from <https://www.arb.ca.gov/ports/shorepower/shorepower.htm>
- Chang, J. C., & Hanna, S. R. (2004). Air quality model performance evaluation. *Meteorology and Atmospheric Physics*, 87(1–3). <https://doi.org/10.1007/s00703-003-0070-7>
- Chen, D., Zhao, N., Lang, J., Zhou, Y., Wang, X., Li, Y., ... Guo, X. (2018). Contribution of ship emissions to the concentration of PM<sub>2.5</sub>: A comprehensive study using AIS data and WRF/Chem model in Bohai Rim Region, China. *Science of The Total Environment*, 610–611, 1476–1486. <https://doi.org/10.1016/j.scitotenv.2017.07.255>
- Chen, W.-W., Gao, R.-L., Liu, L.-S., Zhu, M.-L., Wang, W., Wang, Y.-J., ... Hu, S.-S. (2017). China cardiovascular diseases report 2015: a summary. *Journal of Geriatric Cardiology: JGC*, 14(1), 1–10. <https://doi.org/10.11909/j.issn.1671-5411.2017.01.012>
- Corbett, J., Fischbeck, P., Pandis, S., 1999. Global nitrogen and sulphur inventories for oceangoing ships. *J. Geophys. Res.* 104:3457e3470. <http://dx.doi.org/10.1029/1998JD100040>.
- Corbett, J. J., Winebrake, J. J., Green, E. H., Kasibhatla, P., Eyring, V., & Lauer, A. (2007). Mortality from Ship Emissions: A Global Assessment. *Environmental Science & Technology*, 41(24), 8512–8518. <https://doi.org/10.1021/es071686z>
- Emmons, L. K., Walters, S., Hess, P. G., Lamarque, J.-F., Pfister, G. G., Fillmore, D., ... Kloster, S. (2010). Description and evaluation of the Model for Ozone and Related chemical Tracers, version 4 (MOZART-4). *Geosci. Model Dev.*, 3(1), 43–67. <https://doi.org/10.5194/gmd-3-43-2010>
- Environmental Systems Research Institute (ESRI). (2012). ArcGIS Release 10.1. Redlands, CA.
- Eyring, V., Isaksen, I. S. A., Berntsen, T., Collins, W. J., Corbett, J. J., Endresen, O., ... Stevenson, D. S. (2010). Transport impacts on atmosphere and climate: Shipping. *Atmospheric Environment*, 44(37), 4735–4771. <https://doi.org/10.1016/j.atmosenv.2009.04.059>
- Grell, G. A., Peckham, S. E., Schmitz, R., McKeen, S. A., Frost, G., Skamarock, W. C., and Eder, B.: Fully coupled “online” chemistry within the WRF model, *Atmos. Environ.*, 39, 6957–6975, doi: 10.1016/j.atmosenv.2005.04.027, 2005.

- Gong, S. L.: A parameterization of sea-salt aerosol source function for sub- and super-micron particles, *Global Biogeochem. Cy.*, 17, 1097, doi:10.1029/2003GB002079, 2003.
- Guenther, A. B., Jiang, X., Heald, C. L., Sakulyanontvittaya, T., Duhl, T., Emmons, L. K., and Wang, X.: The Model of Emissions of Gases and Aerosols from Nature version 2.1 (MEGAN2.1): an extended and updated framework for modeling biogenic emissions, *Geosci. Model Dev.*, 5, 1471–1492, doi:10.5194/gmd-5-1471-2012, <http://www.geosci-model-dev.net/5/1471/2012/>, 2012.
- Huang, R., J. Chen, L. Wang, and Z. Lin. 2012. Characteristics, processes, and causes of the spatiotemporal variabilities of the East Asian monsoon system. *Advances in Atmospheric Sciences* 29(5): 910–942.
- Janssens-Maenhout, G., Crippa, M., Guizzardi, D., Dentener, F., Muntean, M., Pouliot, G., Keating, T., Zhang, Q., Kurokawa, J., Wankmüller, R., Denier van der Gon, H., Kuenen, J. J. P., Klimont, Z., Frost, G., Darras, S., Koffi, B., and Li, M.: HTAP\_v2.2: a mosaic of regional and global emission grid maps for 2008 and 2010 to study hemispheric transport of air pollution, *Atmospheric Chemistry and Physics*, 15, 11 411–11 432, doi:10.5194/acp-15-11411-2015, <http://www.atmos-chem-phys.net/15/11411/2015/>, 2015.
- Jeong, Ju-Hee & Shon, Zang-Ho & Kang, Minsung & Song, Sang-Keun & Kim, Yoo-Keun & Park, Jinsoo & Kim, Hyunjae. (2017). Comparison of source apportionment of PM<sub>2.5</sub> using receptor models in the main hub port city of East Asia: Busan. *Atmospheric Environment*. 148. 115-127. 10.1016/j.atmosenv.2016.10.055.
- Jerrett, M., Burnett, R. T., Pope, C. A., Ito, K., Thurston, G., Krewski, D., ... Thun, M. (2009). Long-Term Ozone Exposure and Mortality. *New England Journal of Medicine*, 360(11), 1085–1095. <https://doi.org/10.1056/NEJMoa0803894>
- Kurokawa, J., Ohara, T., Morikawa, T., Hanayama, S., Janssens- Maenhout, G., Fukui, T., Kawashima, K., and Akimoto, H.: Emissions of air pollutants and greenhouse gases over Asian regions during 2000–2008: Regional Emission inventory in ASia (REAS) version 2, *Atmos. Chem. Phys.*, 13, 11019–11058, doi:10.5194/acp-13-11019-2013, 2013.
- Lin, H., Liu, T., Xiao, J., Zeng, W., Li, X., Guo, L., Zhang, Y., Xu, Y., Tao, J., Xian, H., Syberg, K. M., Qian, Z. and Ma, W. (2016) 'Mortality burden of ambient fine particulate air pollution in six Chinese cities: Results from the Pearl River Delta study', *Environment International*, 96, pp. 91-97.
- Liu, H., Fu, M.L., Jin, X.X., Shang, Y., Shindell, D., Faluvegi, G., Shindell, C., He, K.B., 2016. Health and climate impacts of ocean-going vessels in East Asia. *Nat. Clim. Chang.* 6 (11). <http://dx.doi.org/10.1038/NCLIMATE3083> (1037-+).
- Liu, H., Jin, X., Wu, L., Wang, X., Fu, M., Lv, Z., ... He, K. (2018). The impact of marine shipping and its DECA control on air quality in the Pearl River Delta, China. *Science of The Total Environment*, 625, 1476–1485. <https://doi.org/10.1016/j.scitotenv.2018.01.033>
- Lu, X., Chow, K.C., Yao, T., et al., 2009. Seasonal variation of the land sea breeze circulation in the Pearl River Delta Region. *J. Geophys. Res. Atmos.* 114 (D17).
- Lv, Z., Liu, H., Ying, Q., Fu, M., Meng, Z., Wang, Y., ... He, K. (2018). Impacts of shipping emissions on PM<sub>2.5</sub> air pollution in China. *Atmospheric Chemistry and Physics Discussions*, 1–27. <https://doi.org/10.5194/acp-2018-540>

- Ministry of Transport of the People's Republic of China. (2016). 2015 Transport Industry Statistical Communiqué. Retrieved from [http://zizhan.mot.gov.cn/zfxxgk/bnssj/zhghs/201605/t20160506\\_2024006.html](http://zizhan.mot.gov.cn/zfxxgk/bnssj/zhghs/201605/t20160506_2024006.html)
- National Centers for Environmental Prediction and National Weather Service NOAA U. S. Department of Commerce, NCEP FNL Operational Model Global Tropospheric Analyses, continuing from July 1999. 2000.
- NCEI, NOAA. National Centers for Environmental Information (NCEI), <http://gis.ncdc.noaa.gov/maps/ncei/cdo/hourly>
- The NCAR Command Language (Version 6.4.0) [Software]. (2017). Boulder, Colorado: UCAR/NCAR/CISL/TDD. <http://dx.doi.org/10.5065/D6WD3XH5>
- Olmer, N., Comer, B., Roy, B., Mao, X., & Rutherford, D. (2017). Greenhouse gas emissions from global shipping, 2013–2015, 38.
- Ortega, James M., 1932-. (1994). An introduction to Fortran 90 for scientific computing. Fort Worth :Saunders College Pub.
- Paul Campling and Liliane Janssen (VITO)., Kris Vanherle (TML)., Janusz Cofala., Chris Heyes., and Robert Sander (IIASA), 2013. Specific Evaluation of Emissions From Shipping Including Assessment for the Establishment of Possible New Emission Control Areas in European Seas. <http://ec.europa.eu/environment/air/pdf/Main%20Report%20Shipping.pdf>.
- QGIS Development Team, 2009. QGIS Geographic Information System. Open Source Geospatial Foundation. URL <http://qgis.osgeo.org>
- R Core Team (2013). R: A language and environment for statistical computing. R Foundation for Statistical Computing, Vienna, Austria. URL <http://www.R-project.org/>.
- Research Systems, Inc. (1995). IDL user's guide : interactive data language version 4. Boulder, CO :Research Systems,
- Rossum, G. (1995). Python Reference Manual. Amsterdam, The Netherlands, The Netherlands: CWI (Centre for Mathematics and Computer Science).
- Schell, B., Ackermann, I. J., Hass, H., Binkowski, F. S., and Ebel, A.: Modeling the formation of secondary organic aerosol within a comprehensive air quality model system, *J. Geophys. Res.- Atmos.*, 106, 28275–28293, 2001.
- Shaw, W. J., Jerry Allwine, K., Fritz, B. G., Rutz, F. C., Rishel, J. P., and Chapman, E. G.: An evaluation of the wind erosion module in DUSTRAN, *Atmos. Environ.*, 42, 1907–1921, doi:10.1016/j.atmosenv.2007.11.022, 2008.
- T. W. P. Smith, J. P. Jalkanen, B. A. Anderson, J. J. Corbett, J. Faber, S. Hanayama, E. O'Keeffe, S. Parker, L. Johansson, L. Aldous, C. Raucci, M. Traut, S. Ettinger, D. Nelissen, D. S. Lee, S. Ng, A. Agrawal, J. J. Winebrake, M. Hoen, S. Chesworth and A. Pandey, Third IMO GHG Study 2014, Tech. rep., International Maritime Organization (IMO), London, UK, 2014, p. 327.
- Sofiev, M., Winebrake, J. J., Johansson, L., Carr, E. W., Prank, M., Soares, J., ... Corbett, J. J. (2018). Cleaner fuels for ships provide public health benefits with climate tradeoffs. *Nature Communications*, 9(1), 406. <https://doi.org/10.1038/s41467-017-02774-9>
- Stockwell, W. R., Middleton, P., Chang, J. S., and Tang, X.: The second generation regional acid deposition model chemical mechanism for regional air quality modeling, *J. Geophys. Res.-Atmos.*, 95, 16343–16367, doi:10.1029/JD095iD10p16343, 1990.
- Tao, Y., Huang, W., Huang, X., Zhong, L., Lu, S.-E., Li, Y., Dai, L., Zhang, Y. and Zhu, T. (2012) 'Estimated Acute Effects of Ambient Ozone and Nitrogen Dioxide on Mortality

- in the Pearl River Delta of Southern China', *Environmental Health Perspectives*, 120(3), pp. 393-398.
- Tao, J., Zhang, L.M., Cao, J.J., Zhong, L.J., Chen, D.S., Yang, Y.H., Chen, D.H., Chen, L.G., Zhang, Z.S., Wu, Y.F., Xia, Y.J., Ye, S.Q., Zhang, R.J., 2017. Source apportionment of PM<sub>2.5</sub> at urban and suburban areas of the Pearl River Delta region, south China - with emphasis on ship emissions. *Sci. Total Environ.* 574:1559–1570. <http://dx.doi.org/10.1016/j.scitotenv.2016.08.175>.
- Tian, L., Ho, K., Louie, P. K. K., Qiu, H., Pun, V. C., Kan, H., ... Wong, T. W. (2013). Shipping emissions associated with increased cardiovascular hospitalizations. *Atmospheric Environment*, 74, 320–325. <https://doi.org/10.1016/j.atmosenv.2013.04.014>
- United Nations Conference on Trade and Development. (2017). Review of Maritime Transport 2017. Retrieved from [http://unctad.org/en/PublicationsLibrary/rmt2018\\_en.pdf](http://unctad.org/en/PublicationsLibrary/rmt2018_en.pdf).
- US EPA, 2009. Integrated Science Assessment for Particulate Matter (final report). Research Triangle Park (Dec.).
- Viana, M., Hammingh, P., Colette, A., Querol, X., Degraeuwe, B., Vlioger, I. de, & van Aardenne, J. (2014). Impact of maritime transport emissions on coastal air quality in Europe. *Atmospheric Environment*, 90, 96–105. <https://doi.org/10.1016/j.atmosenv.2014.03.046>
- WHO, 2013. Review of evidence on health aspects of air pollution — REVIHAAP Copenhagen.
- Wiedinmyer, C., Akagi, S. K., Yokelson, R. J., Emmons, L. K., Al-Saadi, J. A., Orlando, J. J., and Soja, A. J.: The Fire INventory from NCAR (FINN): a high resolution global model to estimate the emissions from open burning, *Geoscientific Model Development*, 4, 625–641, doi:10.5194/gmd-4-625-2011, <http://www.geosci-model-dev.net/4/625/2011/>, 2011.
- Wild, O., Zhu, X., and Prather, M.: Fast-J: Accurate Simulation of In- and Below-Cloud Photolysis in Tropospheric Chemical Models, *J. Atmos. Chem.*, 37, 245–282, doi:10.1023/A:1006415919030, 2000.
- Winebrake, J. J., Corbett, J. J., Green, E. H., Lauer, A., & Eyring, V. (2009). Mitigating the Health Impacts of Pollution from Oceangoing Shipping: An Assessment of Low-Sulfur Fuel Mandates. *Environmental Science & Technology*, 43(13), 4776–4782. <https://doi.org/10.1021/es803224q>
- WSC (World Shipping Council) (2014). Top 50 World Container Ports. <http://www.worldshipping.org/about-the-industry/global-trade/top-50-worldcontainer-ports> (accessed 20 August 2018).
- Yau, P.S., Lee, S.C., Cheng, Y., Huang, Y., Lai, S.C., Xu, X.H., 2013. Contribution of ship emissions to the fine particulate in the community near an international port in Hong Kong. *Atmos. Res.* 124:61–72.
- Zhang, Y., Yang, X., Brown, R., Yang, L.P., Morawska, L., Ristovski, Z., Fu, Q.Y., Huang, C., 2017. Shipping emissions and their impacts on air quality in China. *Sci. Total Environ.* 581:186–198. <http://dx.doi.org/10.1016/j.sdtotenv.2016.12.098>.
- Zhu, J., 2016. China Ports Year Book. 486. China Ports, Beijing, China.

## 7. Tables

Table 1 Scenarios used for ship emissions.

Scenario	Name	Description	Emission control policies for ships
S0	<i>Baseline</i>	All land emissions	

S1	<i>2015 With Ship</i>	All land emissions plus 2015 ship emissions	PM & SO <sub>2</sub> : None NO <sub>x</sub> : Tier II ship engine
S2	<i>2030 BAU</i>	All land emissions plus 2030 business as usual (BAU) ship emissions	PM & SO <sub>2</sub> : Global: IMO sulfur cap China: DECA 2.0 NO <sub>x</sub> : Tier II ship engine
S3	<i>2030 ECA</i>	All land emissions plus 2030 emission control area (ECA) implemented ship emissions	PM & SO <sub>2</sub> : Global: IMO sulfur cap China: ECA NO <sub>x</sub> : Tier III ship engine for ships built after 2025

Table 2 The IMO NO<sub>x</sub> Tier emission regulations.

IMO Tier	Ship construction date on or after	Total weighted cycle emission limit (g/kWh) n = engine's rated speed (rpm)		
		n < 130	130 < n < 1999	n ≥ 2000
I	1 January 2000	17.0	$45 \times n \times (-0.2)$	9.8
II	1 January 2011	14.4	$44 \times n \times (-0.23)$	7.7

III	1 January 2016 * Only when operating in the North American ECA	3.4	$9 \times n \times (-0.2)$	2.0

Table 3 Scale factors of emission factors, by pollutant type.

Pollutant	SF in 2030, BAU	SF in 2030, BAU special zones	SF in 2030, ECA
SO <sub>x</sub>	0.2	0.04	0.04
PM	0.5 on average	0.1 on average	0.1 on average

NO <sub>x</sub>	0.9 on average	0.22 on average	0.22 on average
CO <sub>2</sub>	1	1	1
CO	1	1	1
BC	1	0.25	0.25
CH <sub>4</sub>	1	1	1
N <sub>2</sub> O	1	0.94	0.94
NMVOC	1	1	1

Table 4 Health outcomes and risk functions used to calculate the burden of diseases associated with the exposure to PM<sub>2.5</sub> and O<sub>3</sub>.

<b>Outcome and exposure metric</b>	<b>Relative Risks (95% CI)</b>	<b>Reference</b>
All cause (natural) mortality from short-term exposure to PM <sub>2.5</sub>	1.0176 (1.0147, 1.0206)	Lin et al., 2016
Cardiovascular (CVD) mortality from short-term exposure to PM <sub>2.5</sub>	1.0219 (1.0180, 1.0259)	Lin et al., 2016
Respiratory mortality from short-term exposure to PM <sub>2.5</sub>	1.0168 (1.010, 1.0237)	Lin et al., 2016

All cause (natural) mortality from short-term exposure to O <sub>3</sub>	1.0081 (1.0063, 1.010)	Tao et al., 2012
Cardiovascular (CVD) mortality from short-term exposure to O <sub>3</sub>	1.0101 (1.0071, 1.0132)	Tao et al., 2012
Respiratory mortality from short-term exposure to O <sub>3</sub>	1.0133 (1.0089, 1.0176)	Tao et al., 2012
Ischemic heart disease (IHD) from long-term exposure to PM <sub>2.5</sub>	IER * Depends on specific concentrations and group ages.	2015 GBD study
Chronic obstructive pulmonary disease (COPD) from long-term exposure to PM <sub>2.5</sub>		
Cerebrovascular disease (CEV) from long-term exposure to PM <sub>2.5</sub>		
Lung cancer (LC) from long-term exposure to PM <sub>2.5</sub>		
Respiratory mortality from long-term exposure to PM <sub>2.5</sub>	1.009 (0.982, 1.04)	Cao et al., 2011
Ischemic heart disease (IHD) from long-term exposure to O <sub>3</sub>	1.015 (1.003, 1.026)	Jerret et al., 2009
Respiratory mortality from long-term exposure to O <sub>3</sub>	1.029 (1.010, 1.048)	Jerret et al., 2009
Cardiovascular (CVD) mortality from long-term exposure to O <sub>3</sub>	1.011 (1.003, 1.023)	Jerret et al., 2009

Table 5 Summary emissions for four scenarios in the model.

Unit: (kt/year)	Baseline		Ship emissions within 200 nm ECA		
	China	PRD	2015	2030 BAU	2030 ECA
PM <sub>2.5</sub>	9236.8	158.2	11.3	9.9	4.3
SO <sub>2</sub>	18335.3	350.3	89.5	27.0	6.4
NO <sub>x</sub>	25701.7	669.3	141.9	197.9	172.3

Table 6 Summary statistics for the four meteorological variables (temperature, wind speed, wind direction, relative humidity) between modeled and observed in four cities of the PRD region.

Variable	Site	NMB(%)	NME(%)	MFB(%)	MFE(%)	r	RMSE
2-meter Temperature	Guangzhou	0.3	0.3	0.1	0.1	0.9	1.2
	Shenzhen	0.2	0.3	0.1	0.1	0.8	1.1
	Zhaoqing	-0.3	0.4	-0.1	0.1	0.7	1.6
	Hong Kong	0.0	0.2	0.0	0.1	0.8	0.9
10-meter Wind Speed	Guangzhou	-15.0	17.6	-4.4	5.1	0.9	0.6
	Shenzhen	-36.4	36.4	-11.2	11.2	0.8	2.0
	Zhaoqing	31.6	39.9	5.9	8.0	0.5	1.0

	Hong Kong	-35.9	35.9	-11.0	11.0	0.8	1.9
10-meter Wind Direction	Guangzhou	-9.8	21.0	-2.7	5.6	0.5	45.7
	Shenzhen	-0.8	11.9	-0.7	3.2	0.8	30.7
	Zhaoqing	-5.9	21.1	-0.8	5.6	0.5	47.3
	Hong Kong	11.2	17.8	2.2	4.1	0.6	46.4
Surface Relative Humidity	Guangzhou	-15.9	16.4	-4.7	4.9	0.5	17.0
	Shenzhen	-12.3	15.1	-3.8	4.5	0.6	15.9
	Zhaoqing	-1.6	9.1	-0.6	2.4	0.5	10.1
	Hong Kong	-2.6	11.2	-1.1	3.1	0.7	11.2

Table 7 Summary statistics for four major air pollutant concentrations between modeled and observed in nine major cities of the PRD region.

	City	NMB(%)	NME(%)	MFB(%)	MFE(%)	r	RMSE
PM <sub>2.5</sub>	Guangzhou	193.3	197.4	20.3	21.5	0.5	81.6
	Shenzhen	245.3	245.3	24.3	24.3	0.3	62.6
	Zhuhai	86.6	98.4	10.1	14.5	0.6	26.8
	Foshan	53.6	71.8	7.9	12.4	0.5	36.2
	Zhongshan	195.2	195.3	20.8	20.8	0.4	58.2
	Jiangmen	209.1	211.8	18.7	19.5	0.4	54.1
	Dongguan	188.2	188.2	22.3	22.3	0.5	59.7
	Huizhou	199.5	199.9	24.5	24.6	0.5	49.1

	Zhaoqing	27.2	41.9	4.5	8.5	0.3	18.3
O <sub>3</sub>	Guangzhou	-29.7	40.1	-6.2	10.5	0.5	69.1
	Shenzhen	-5.1	26.6	-0.3	6.1	0.5	37.2
	Zhuhai	-18.6	26.5	-2.9	5.7	0.8	43.4
	Foshan	-27.8	33.1	-7.0	8.6	0.7	53.1
	Zhongshan	-3.8	31.1	1.8	7.7	0.8	34.3
	Jiangmen	1.5	23.9	2.4	6.4	0.8	26.1
	Dongguan	-39.1	40.5	-10.8	11.5	0.7	73.3
	Huizhou	-3.2	19.8	0.0	5.1	0.8	23.2
	Zhaoqing	-26.8	30.5	-7.0	8.1	0.7	43.5
SO <sub>2</sub>	Guangzhou	172.1	190.8	16.7	22.3	0.1	19.2
	Shenzhen	41.2	56.6	3.7	9.1	0.5	7.7
	Zhuhai	14.0	51.1	-4.1	12.7	0.7	4.5
	Foshan	-48.8	49.0	-18.2	18.3	0.7	9.5
	Zhongshan	92.3	111.9	6.1	14.4	0.6	9.9
	Jiangmen	-7.4	66.2	-9.9	18.7	0.3	7.6
	Dongguan	139.3	147.9	17.0	19.3	0.3	13.5
	Huizhou	1.0	53.2	-4.0	13.9	0.1	6.7
	Zhaoqing	-74.2	75.4	-31.7	32.0	0.4	12.2
NO <sub>2</sub>	Guangzhou	-36.7	50.0	-13.1	17.2	0.2	25.2
	Shenzhen	-29.1	43.6	-9.0	12.5	0.4	10.7
	Zhuhai	-66.0	67.4	-27.2	27.6	0.7	14.8
	Foshan	-39.3	48.9	-10.5	15.1	0.7	9.7
	Zhongshan	-32.1	46.4	-12.4	14.9	0.6	11.0
	Jiangmen	-5.2	39.3	-3.6	9.9	0.6	5.9

	Dongguan	-11.1	32.8	-5.2	9.5	0.5	11.0
	Huizhou	24.9	65.4	2.1	13.7	0.1	12.0
	Zhaoqing	-73.6	78.2	-29.8	30.9	-0.1	15.6

Table 8 Monthly average PM<sub>2.5</sub> concentrations for the two scenarios in July 2015: *Baseline Scenario* and *2015 With Ship Scenario* (unit:  $\mu\text{g}/\text{m}^3$ ); the third column shows the increased PM<sub>2.5</sub> concentration due to ships (unit:  $\mu\text{g}/\text{m}^3$ ) and the fourth column shows the percentage of the ambient PM<sub>2.5</sub> concentration was caused by ship (unit: %).

City	Baseline	2015 With Ship PM <sub>2.5</sub>	Ship-caused PM <sub>2.5</sub> Increase	Ship Contribution Among All sources
Jiangmen	31.18	32.25	1.06	3.3%
Shenzhen	91.95	95.96	4.01	4.2%
Guangzhou	72.06	74.21	2.15	2.9%
Foshan	70.02	71.68	1.66	2.3%

Zhuhai	35.86	37.26	1.40	3.8%
Dongguan	73.05	74.11	1.06	1.4%
Zhaoqing	26.54	26.65	0.11	0.4%
Qingyuan	30.21	30.54	0.33	1.1%
Huizhou	29.25	31.55	2.30	7.3%
Heyuan	16.43	17.50	1.07	6.1%
Shaoguan	20.59	21.13	0.54	2.5%
Shanwei	14.87	17.85	2.98	16.7%
Guangdong	31.31	32.41	1.10	3.4%

Table 9 Monthly average O<sub>3</sub> concentrations for the two scenarios in July 2015: *Baseline Scenario* and *2015 With Ship Scenario* (unit: ppb); the third column shows the increased O<sub>3</sub> concentration due to ships (unit: ppb) and the fourth column shows the percentage of the ambient O<sub>3</sub> concentration was caused by ship (unit: %).

City	Baseline	2015 With Ship O <sub>3</sub>	Ship-caused O <sub>3</sub> Increase	Ship Contribution Among All sources
Jiangmen	49.51	51.37	1.86	3.6%
Shenzhen	52.02	55.52	3.50	6.3%
Guangzhou	56.55	58.20	1.65	2.8%

Foshan	57.25	59.01	1.76	3.0%
Zhuhai	49.76	53.98	4.22	7.8%
Dongguan	57.21	58.67	1.46	2.5%
Zhaoqing	47.66	48.38	0.72	1.5%
Qingyuan	51.35	52.04	0.69	1.3%
Huizhou	50.30	53.05	2.75	5.2%
Heyuan	46.47	47.97	1.49	3.1%
Shaoguan	50.92	51.38	0.47	0.9%
Shanwei	39.20	44.98	5.79	12.9%
Guangdong	49.00	50.62	1.62	3.2%

Table 10 The projected 2030 BAU death incidences (unit: cases) and the health benefits (unit: cases and %) brought by the ECA implementation.

PM <sub>2.5</sub>	All cause	IHD	COPD	LC	CEV	Respiratory
2030 BAU Incidence (cases)	1525	474	220	146	653	32
ECA Benefits (cases)	1044	374	162	92	424	20
% Death ECA Reduced	68%	79%	74%	63%	65%	63%
O <sub>3</sub>	All cause	CVD	Respiratory			
2030 BAU Incidence (cases)	1020	966	212			

ECA Benefits (cases)	143	125	18	
% Death ECA Reduced	14%	13%	8%	

## 8. Figures

Figure 1 The flow chart of thesis. The thesis has been finished by three parts: Part 1 Emission, Part 2 Modeling and Part 3 Health Impact.

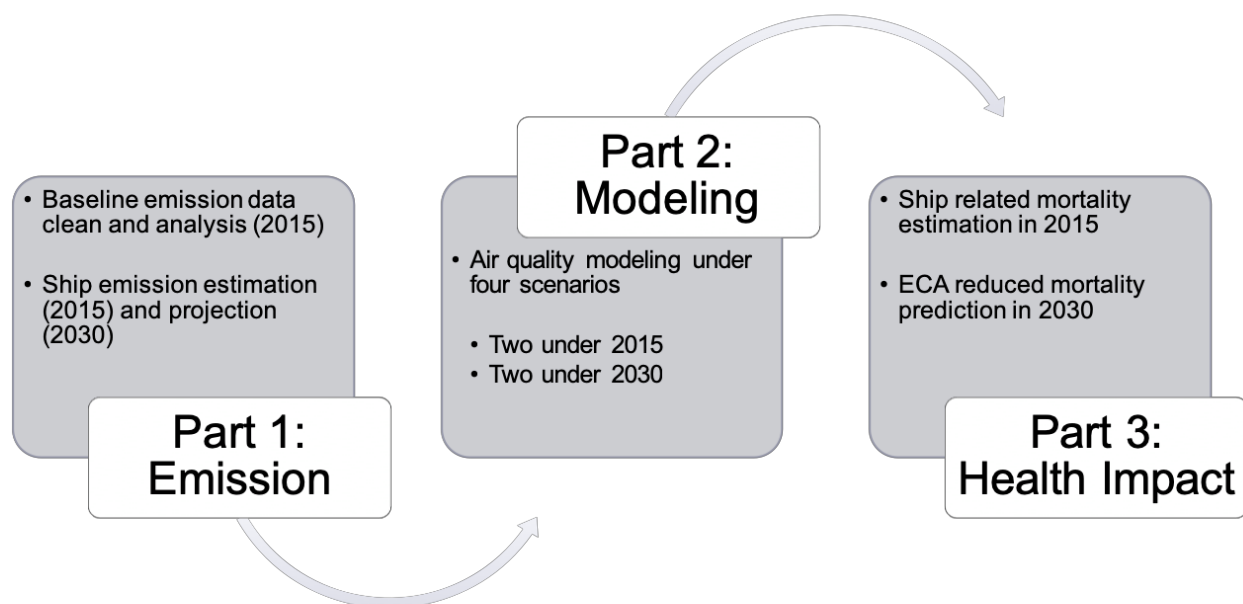


Figure 2 The geographical location of the PRD region (left) and the spatial distribution of ports (black dots), air quality monitoring stations (red) and meteorological stations (blue) inside of the domain 3 (right). The three domain sizes are also shown in the left map. The orange slash area denotes the 200 nm ECA area.

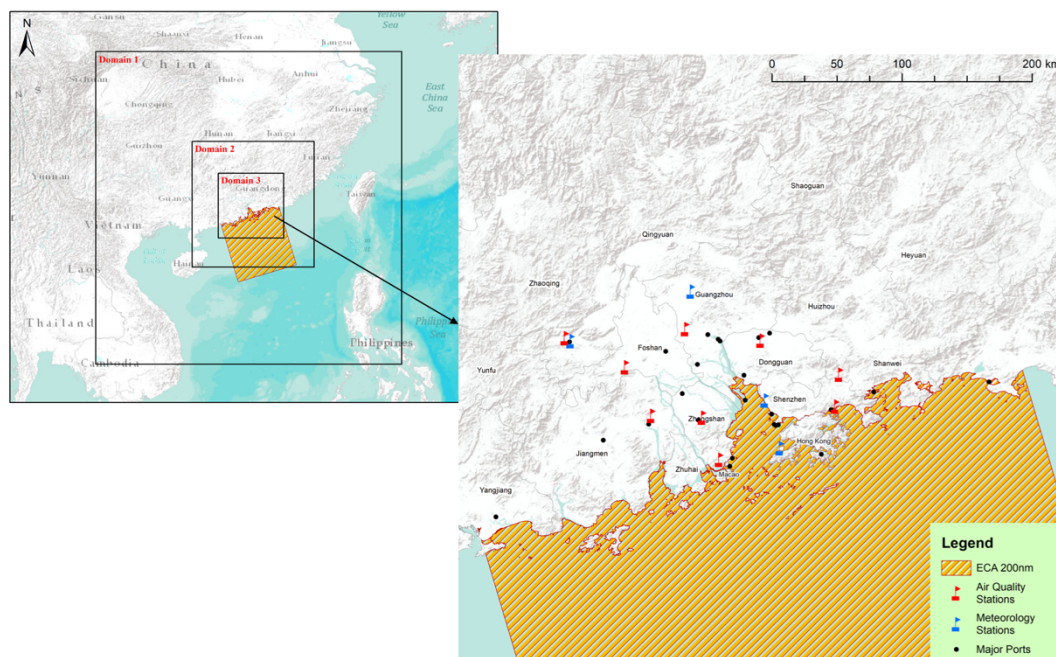


Figure 3 Monthly mean surface emissions of five pollutants ( $PM_{2.5}$ , BC, CO,  $NO_x$ , and  $SO_2$ ) from all sources in July 2015 used in WRF-Chem for the two 2015 simulations.

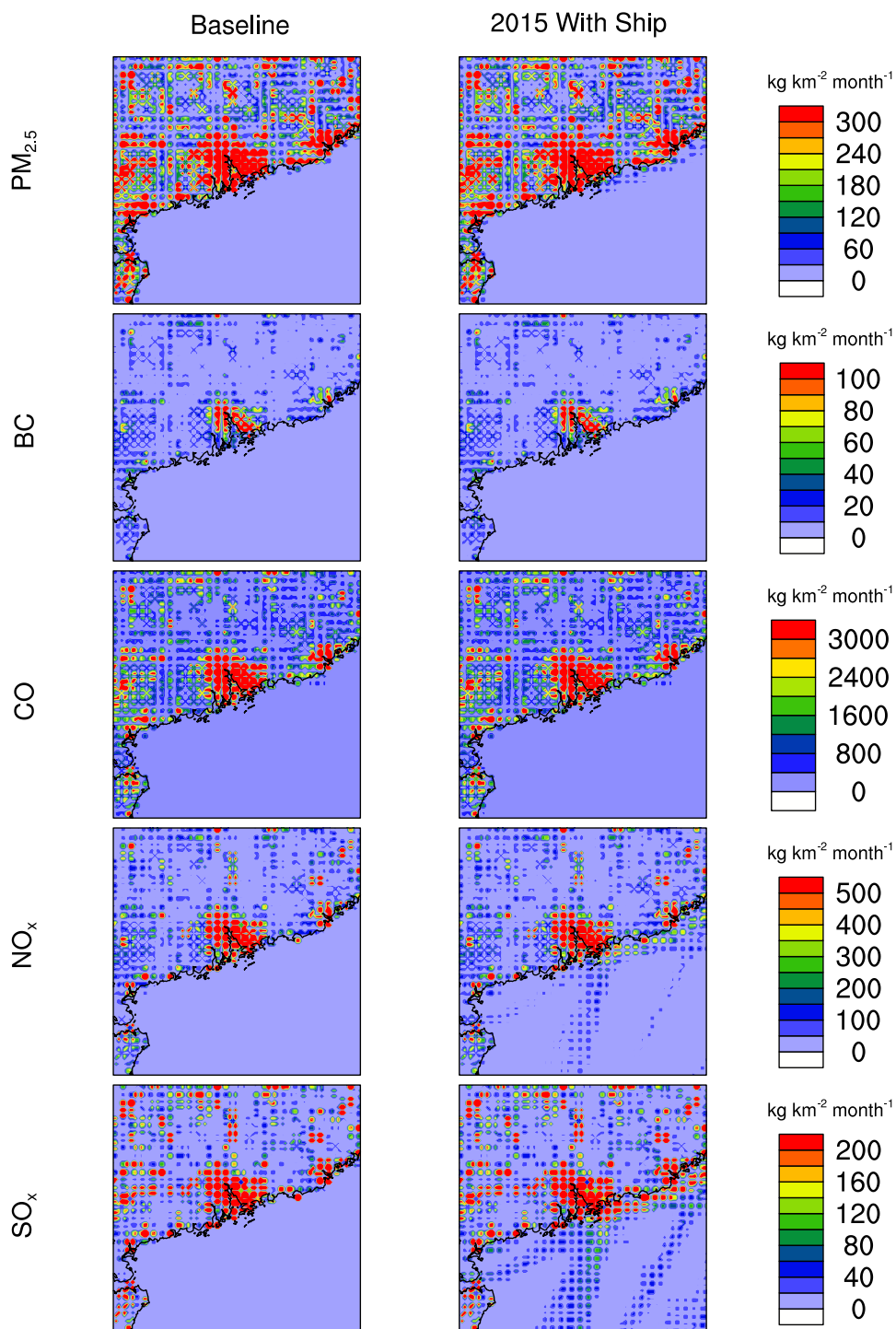


Figure 4 Spatial distribution of PM<sub>2.5</sub>, SO<sub>2</sub>, and NO<sub>x</sub> emissions from ships under the three ship scenarios. (unit: tons/100 km<sup>2</sup>)

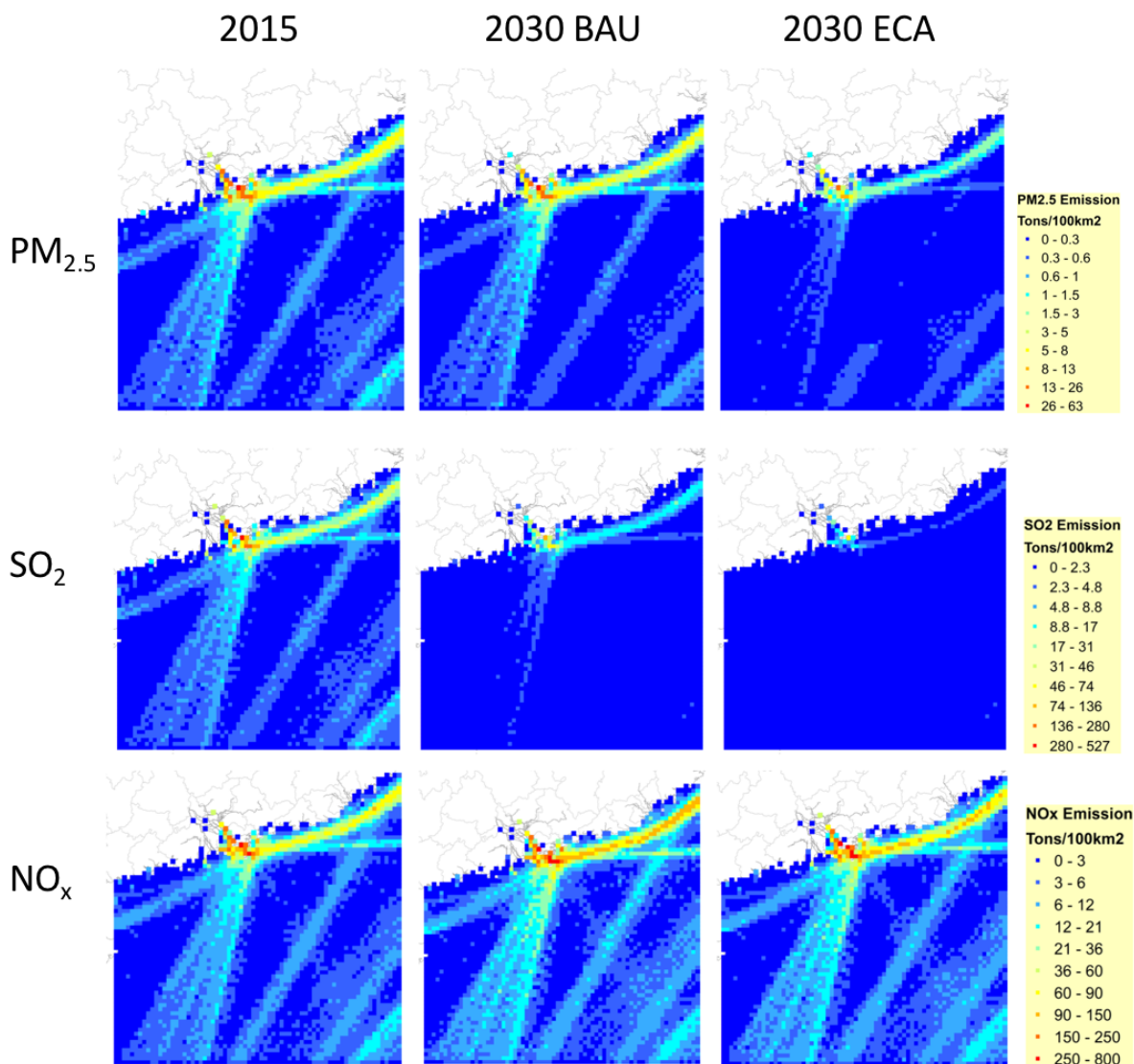


Figure 5 The comparison of wind speed and wind direction between the modeled and observed; the length of each widget shows the number of hours that were observed or modeled within that direction and the color of the widget shows the wind speed for each hour.

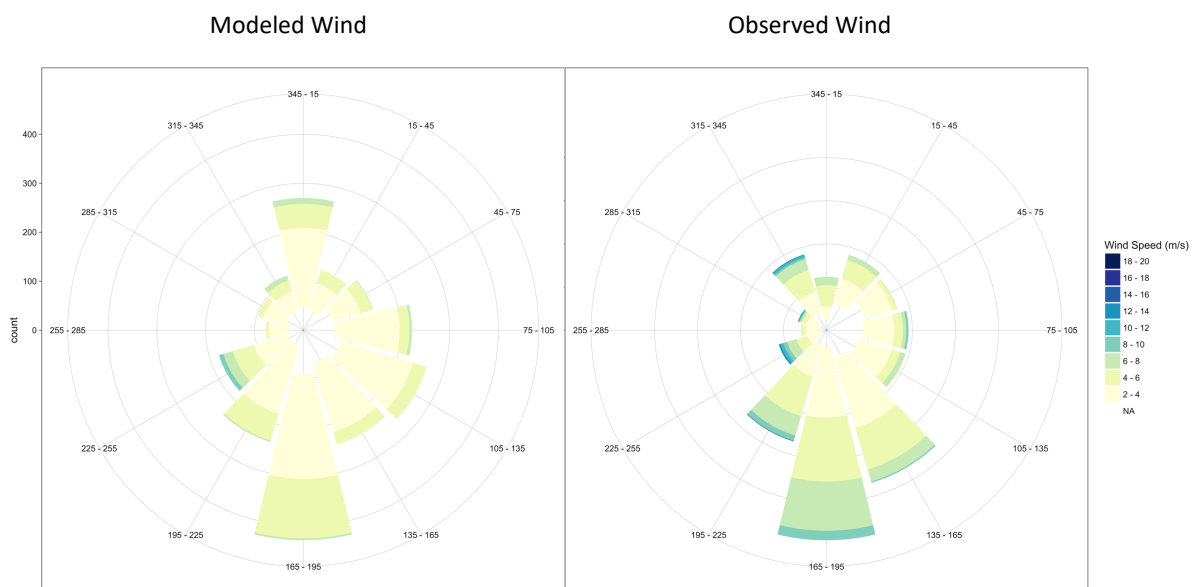


Figure 6 Daily mean  $PM_{2.5}$  and  $O_3$  concentrations between modelled and observed in nine cities.

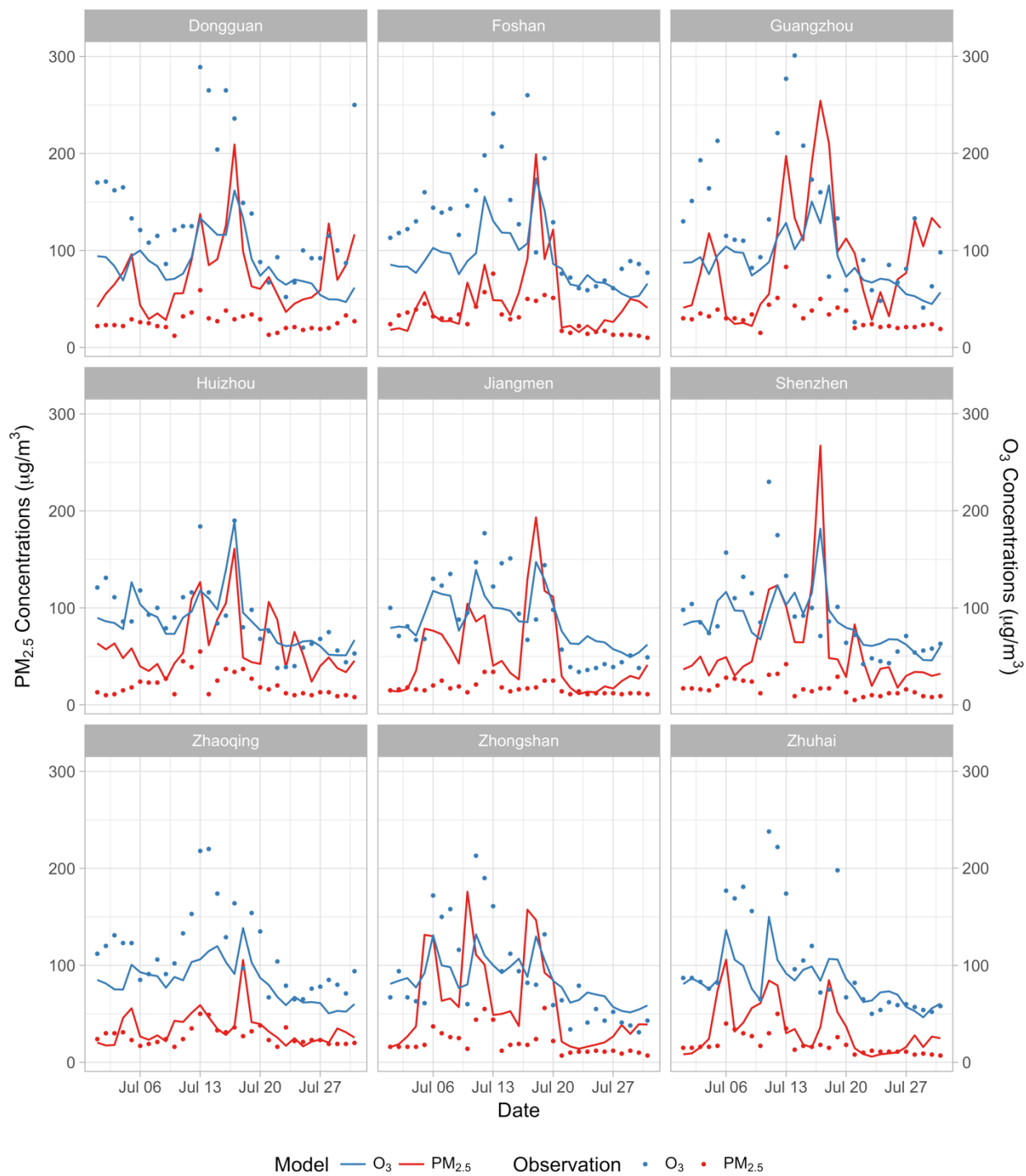


Figure 7 Daily mean  $\text{NO}_2$  and  $\text{SO}_2$  concentrations between modelled and observed in nine cities.

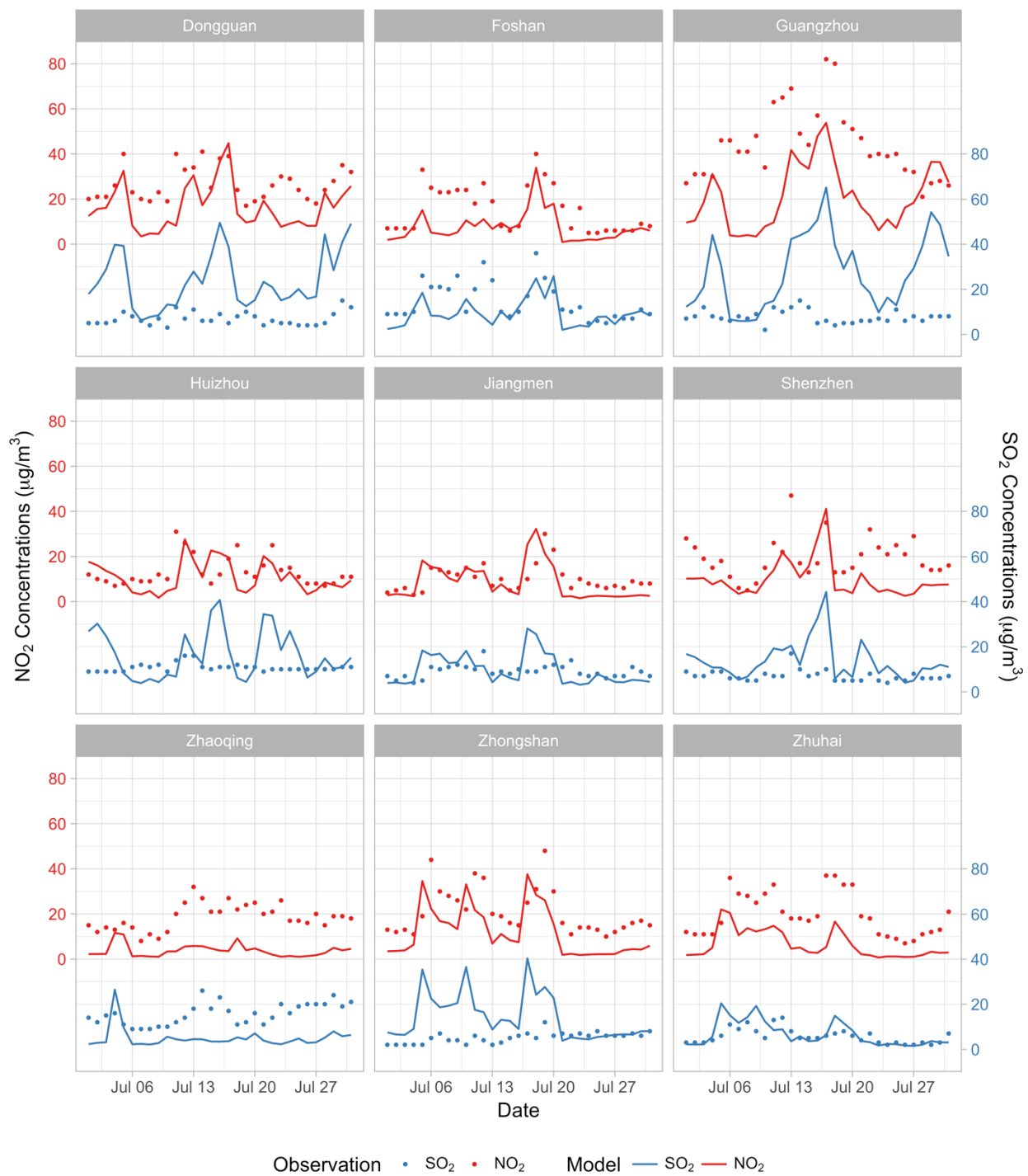


Figure 8 Four pollutant ( $\text{PM}_{2.5}$ ,  $\text{O}_3$ ,  $\text{SO}_2$  and  $\text{NO}_x$ ) concentrations comparing two scenarios in July 2015: *Baseline Scenario* (first column) and *2015 With Ship Scenario* (second column); the increased concentrations due to ship emissions are shown in the third column and the contributions of ship emission compared to other pollution sources are shown in the fourth column.

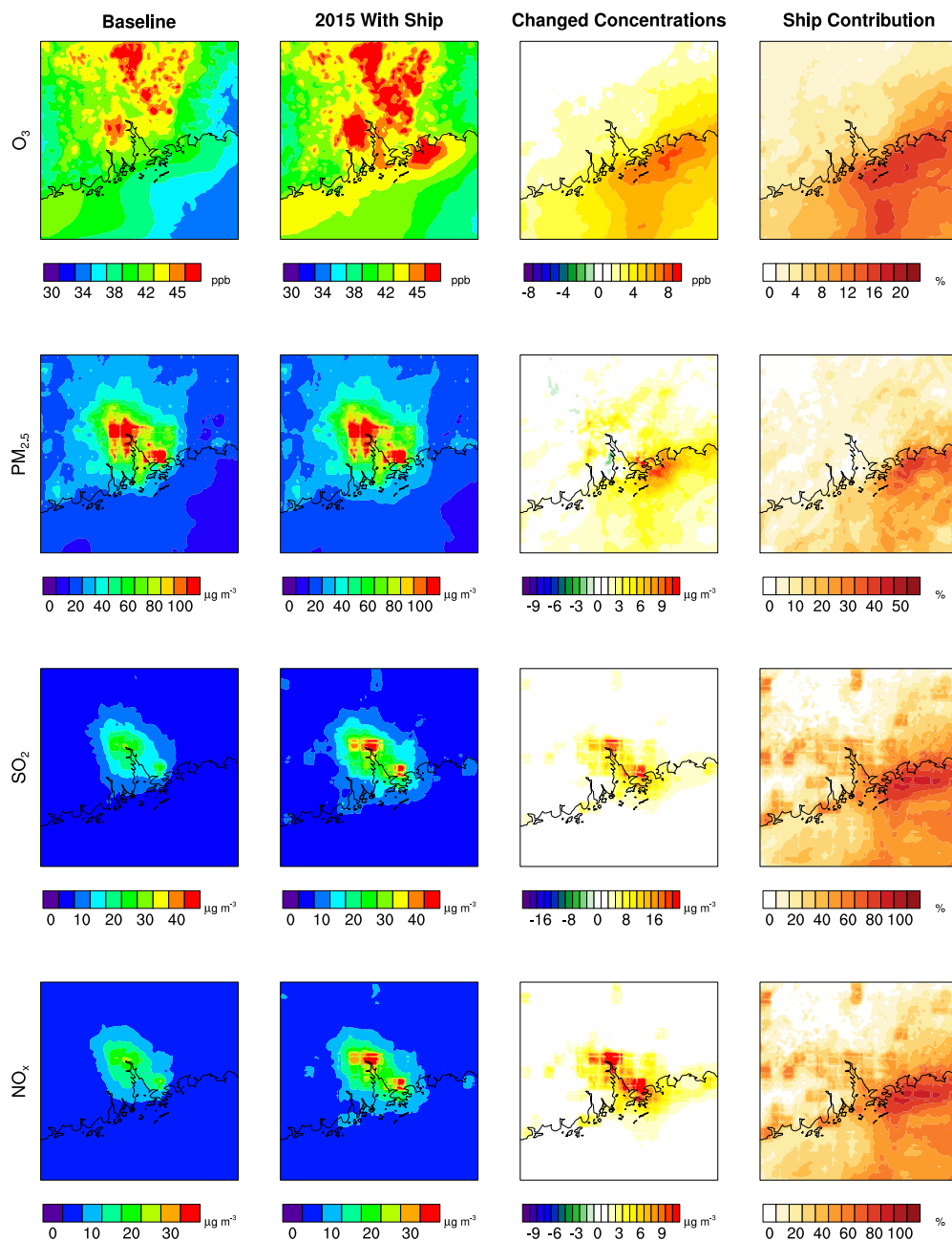


Figure 9 The wind pattern (wind speed [unit: m/s] and wind direction) and temperature (K) under *2015 without ship* scenario (left) and *2015 with ship* scenario (middle) and the changed wind and temperature after adding the ship emissions (right).

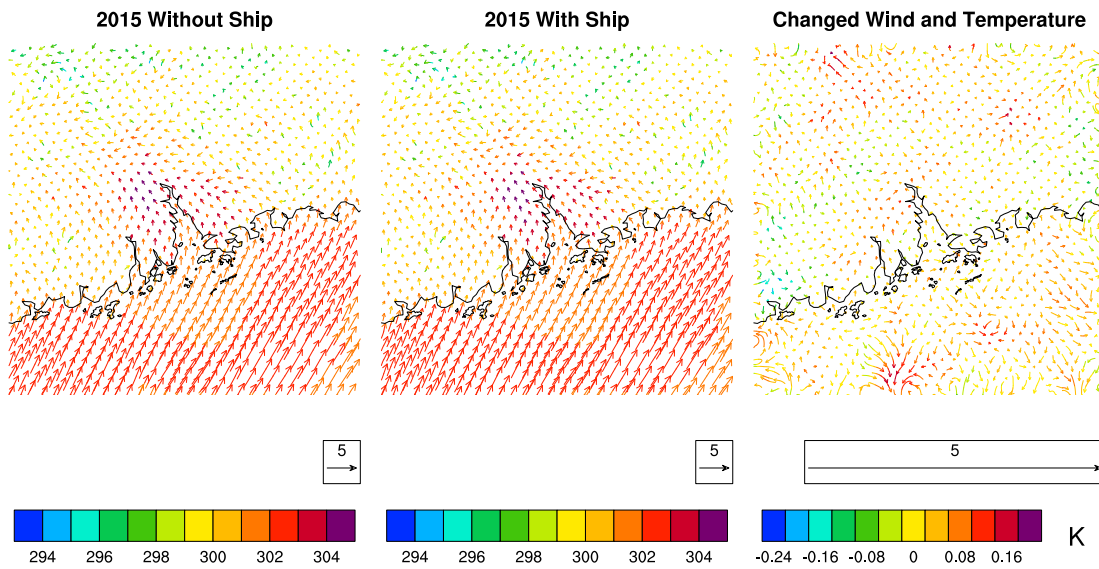


Figure 10 Air quality benefits provided by ECA where the green areas indicate the reduced pollutant concentrations for O<sub>3</sub>, PM<sub>2.5</sub>, SO<sub>2</sub> and NO<sub>x</sub> (units: ppb for O<sub>3</sub> and μg/m<sup>3</sup> for PM<sub>2.5</sub>, SO<sub>2</sub> and NO<sub>x</sub>) after ECA being implemented.

#### ECA Reduced Concentrations

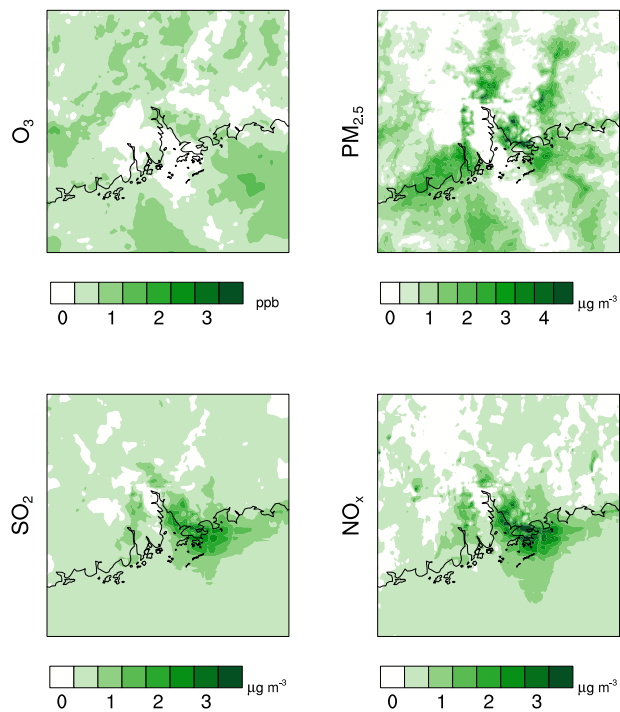


Figure 11 Premature mortality associated with short-term (acute) exposures to ship-related PM<sub>2.5</sub> and O<sub>3</sub> within six major cities in the PRD region; Guangzhou, Shenzhen, and Jiangmen were observed the highest acute mortality incidences.

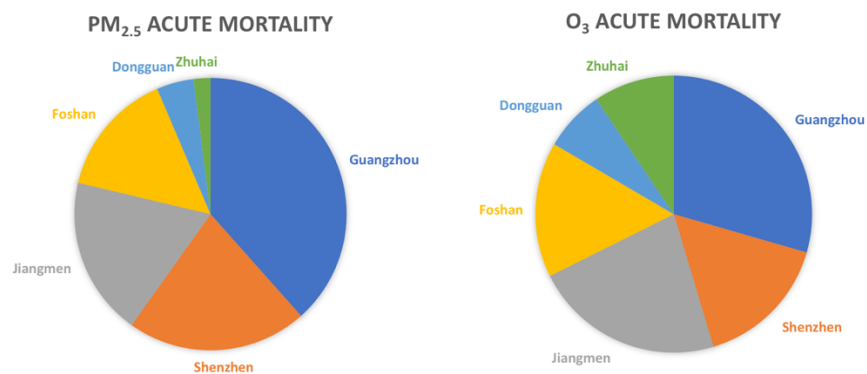


Figure 12 Premature mortality associated with long-term (chronic) exposures to ship-related PM<sub>2.5</sub> in 2015.

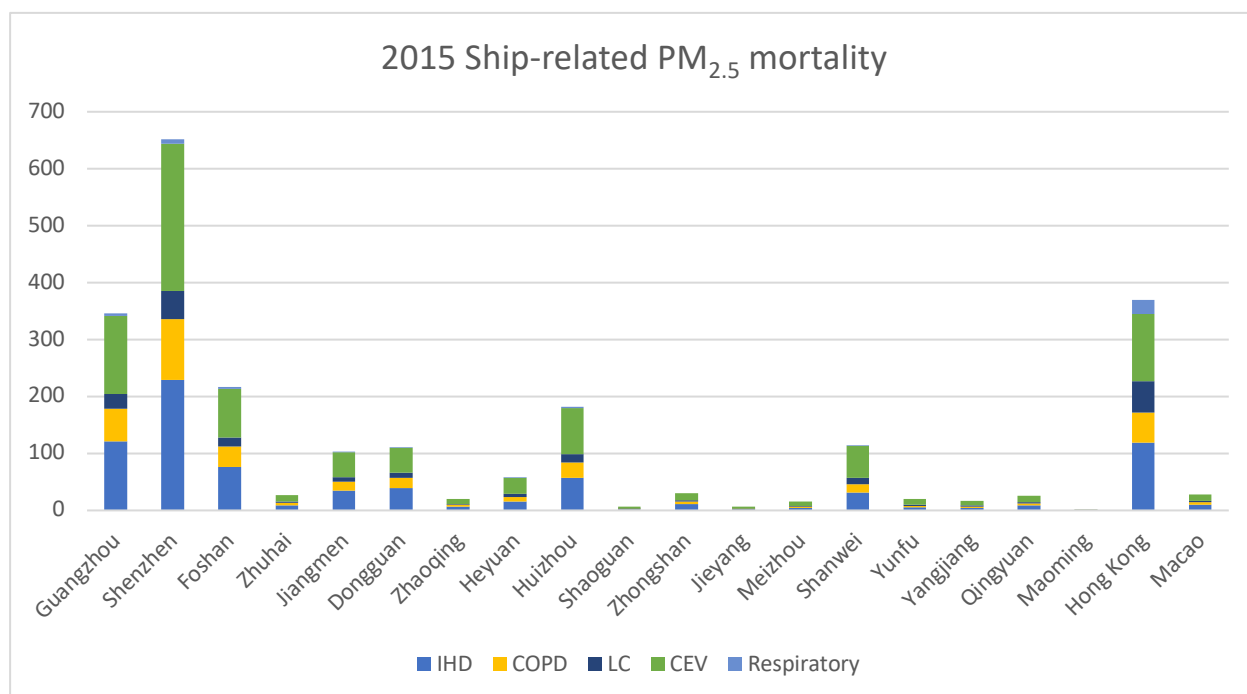


Figure 13 Premature mortality associated with long-term (chronic) exposures to ship-related O<sub>3</sub> in 2015.

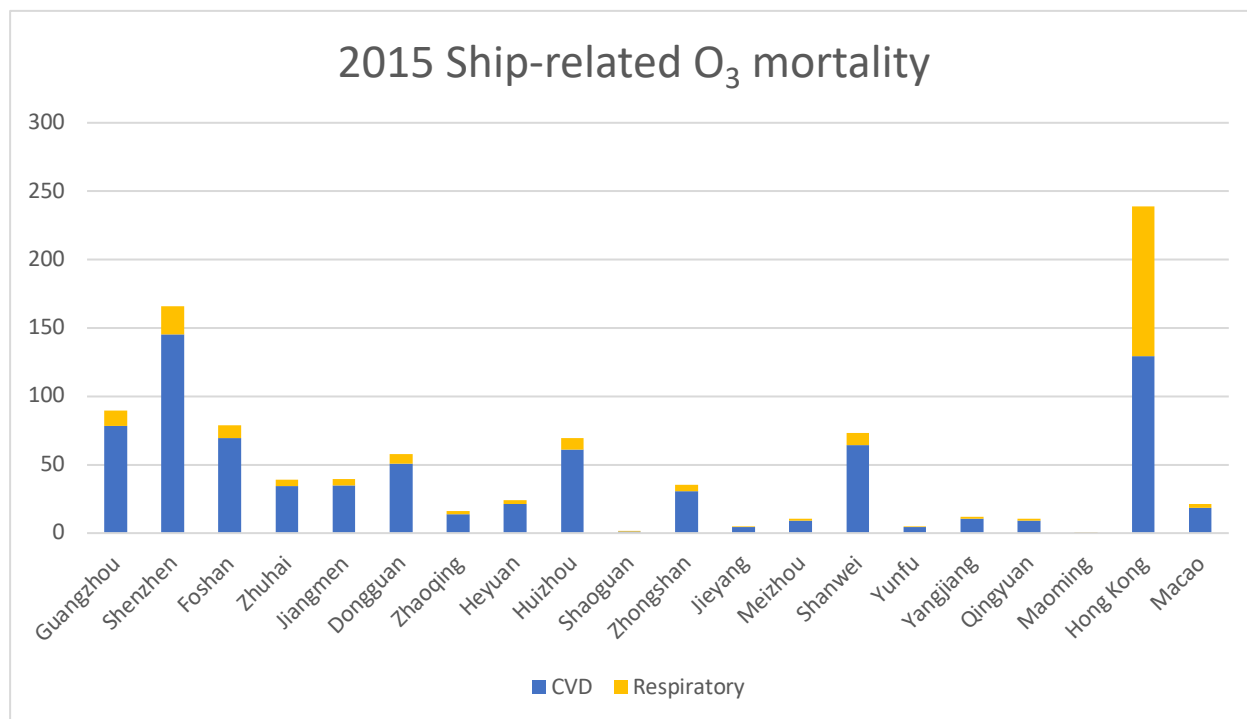


Table S1 Premature mortality associated with short-term (acute) exposures to ship-related PM<sub>2.5</sub> and O<sub>3</sub>.

City	PM2.5									O3								
	All cause			CVD			Respiratory			All cause			CVD			Respiratory		
Guangzhou	60	50	70	30	24	35	9	6	13	34	26	42	17	12	22	9	6	12
Shenzhen	33	28	39	17	14	20	3	2	4	18	14	23	9	7	12	3	2	4
Jiangmen	29	25	34	19	16	23	3	2	4	26	20	32	17	12	22	4	3	6
Foshan	23	19	27	12	10	14	4	2	5	18	14	22	9	7	12	5	3	6
Dongguan	7	6	8	4	4	5	1	0	1	8	6	10	5	4	7	1	1	2
Zhuhai	3	3	4	2	1	2	0	0	0	11	8	13	6	4	8	1	1	2
Six city totals	155	130	181	84	69	99	20	12	28	115	89	142	64	45	83	24	16	31

Table S2 Premature mortality associated with long-term (chronic) exposures to ship-related PM<sub>2.5</sub> in 2015.

City	IHD			COPD			LC			CEV			Respiratory			Total		
	Mean	95% CI: low	95% CI: up	Mean	95% CI: low	95% CI: up	Mean	95% CI: low	95% CI: up									
Guangzhou	122	106	174	57	19	99	26	10	34	137	28	137	4	-8	18	346	155	462
Shenzhen	229	200	326	107	36	185	49	18	64	258	53	260	8	-16	33	651	292	868
Foshan	76	66	109	36	12	62	16	6	21	86	18	86	3	-5	11	217	97	289
Zhuhai	9	8	13	4	1	7	2	1	3	11	2	14	0	-1	1	27	11	37
Jiangmen	35	30	50	16	5	28	8	3	10	44	9	51	1	-2	5	103	46	144
Dongguan	39	34	56	18	6	32	8	3	11	44	9	44	1	-3	6	111	49	148
Zhaoqing	6	6	9	3	1	5	2	1	2	9	2	12	0	0	1	20	9	30
Heyuan	16	14	23	7	3	13	5	1	9	28	7	45	1	-1	2	58	23	91
Huizhou	57	50	82	27	9	47	15	5	21	81	18	106	2	-4	8	182	78	264
Shaoguan	2	2	3	1	0	2	1	0	1	3	1	5	0	0	0	7	3	11
Zhongshan	11	9	15	5	2	9	2	1	3	12	2	12	0	-1	2	30	13	41
Jieyang	2	2	3	1	0	1	1	0	1	3	1	5	0	0	0	7	3	10
Meizhou	4	4	6	2	1	3	2	0	3	8	2	12	0	0	1	15	6	25
Shanwei	31	27	45	15	5	25	11	2	19	56	13	88	1	-2	5	114	46	182
Yunfu	6	5	8	3	1	5	2	0	3	10	2	16	0	0	1	20	9	32
Yangjiang	5	4	7	2	1	4	2	0	2	9	2	13	0	0	1	17	7	28
Qingyuan	8	7	12	4	1	7	2	1	3	11	2	14	0	-1	1	25	11	36
Maoming	0	0	0	0	0	0	0	0	0	0	0	1	0	0	0	1	0	1
Hong Kong	119	104	169	53	18	91	56	18	78	118	27	161	25	-51	109	370	116	608
Macao	10	9	14	5	2	8	2	1	3	11	2	11	0	-1	1	28	12	38
Total	787	687	1123	366	124	634	211	71	290	939	203	1092	46	-96	206	2349	989	3345

Table S3 Premature mortality associated with long-term (chronic) exposures to ship-related O<sub>3</sub> in 2015.

City	CVD	RES	IHD	TOTAL
------	-----	-----	-----	-------

	Mean	95%CI : low	95%CI : up									
Guangzhou	78	17	128	11	3	13	38	8	65	89	20	142
Shenzhen	145	31	238	21	5	25	70	14	120	166	37	262
Foshan	69	15	113	10	2	12	33	7	57	79	17	125
Zhuhai	34	7	56	5	1	6	17	3	28	39	9	62
Jiangmen	35	7	57	5	1	6	17	3	29	40	9	63
Dongguan	51	11	83	7	2	9	24	5	42	58	13	91
Zhaoqing	14	3	23	2	1	2	7	1	12	16	4	25
Heyuan	21	5	35	3	1	4	10	2	18	24	5	38
Huizhou	61	13	99	9	2	10	29	6	50	70	15	110
Shaoguan	1	0	2	0	0	0	1	0	1	2	0	2
Zhongshan	31	7	50	4	1	5	15	3	26	35	8	56
Jieyang	4	1	7	1	0	1	2	0	4	5	1	8
Meizhou	9	2	15	1	0	2	4	1	8	11	2	17
Shanwei	64	14	105	9	2	11	31	6	53	73	16	116
Yunfu	4	1	7	1	0	1	2	0	3	5	1	8
Yangjiang	10	2	17	1	0	2	5	1	9	12	3	19
Qingyuan	9	2	15	1	0	2	4	1	8	10	2	16
Maoming	0	0	1	0	0	0	0	0	0	0	0	1
Hong Kong	129	28	211	110	28	131	60	12	103	239	56	342
Macao	18	4	30	3	1	3	9	4	15	21	5	33
Total	791	171	1292	203	52	243	378	78	650	994	223	1534

Table S4 Projected premature mortality associated with long-term (chronic) exposures to ship-related PM<sub>2.5</sub> in 2030 under BAU scenario.

City	IHD	COPD	LC	CEV	Respiratory	Total
------	-----	------	----	-----	-------------	-------



Guangzhou	101	22	166	14	4	17	49	10	84	105	39	214
Shenzhen	164	35	268	23	6	28	79	16	136	170	63	347
Foshan	71	15	116	10	3	12	34	7	59	74	27	151
Zhuhai	38	8	61	5	1	6	18	4	31	39	14	80
Jiangmen	46	10	74	6	2	8	22	4	38	47	18	96
Dongguan	73	16	119	10	3	12	35	7	60	75	28	154
Zhaoqing	33	7	55	5	1	6	16	3	28	35	13	71
Heyuan	40	9	66	6	1	7	19	4	33	42	15	85
Huizhou	85	18	138	12	3	14	41	8	70	88	33	179
Shaoguan	5	1	8	1	0	1	2	0	4	5	2	10
Zhongshan	37	8	60	5	1	6	18	4	31	38	14	78
Jieyang	6	1	10	1	0	1	3	1	5	6	2	13
Meizhou	24	5	39	3	1	4	11	2	20	25	9	50
Shanwei	65	14	105	9	2	11	31	6	53	67	25	136
Yunfu	14	3	24	2	1	2	7	1	12	15	6	31
Yangjiang	16	3	26	2	1	3	8	2	13	16	6	33
Qingyuan	24	5	38	3	1	4	11	2	19	24	9	50
Maoming	1	0	1	0	0	0	0	0	0	1	0	1
Hong Kong	106	23	173	90	23	108	49	10	84	129	130	222
Macao	19	4	31	3	1	3	9	4	16	20	7	40
Total	966	208	1578	212	54	253	463	95	796	1020	461	2041

Table S6 Avoided premature mortality associated with long-term (chronic) exposures to ship-related PM<sub>2.5</sub> due to implementing the ECA.

City	IHD			COPD			LC			CEV			Respiratory			Total		
	Mean	95% CI: low	95% CI: up	Mean	95% CI: low	95% CI: up	Mea n	95% CI: low	95% CI: up									
Guangzhou	35	31	52	17	6	30	8	3	10	40	8	41	1	-2	5	100	45	138
Shenzhen	107	93	158	50	17	90	23	9	31	121	25	125	4	-7	16	305	136	420
Foshan	23	20	34	11	4	19	5	2	7	26	5	27	1	-2	3	65	29	90
Zhuhai	6	5	8	3	1	5	1	0	2	8	2	11	0	0	1	18	8	27

Jiangmen	31	27	45	14	5	26	7	2	11	44	10	60	1	-2	5	97	42	146
Dongguan	25	22	38	12	4	21	5	2	7	29	6	30	1	-2	4	72	32	100
Zhaoqing	4	4	6	2	1	4	1	0	2	6	1	9	0	0	1	14	6	22
Heyuan	9	8	14	4	1	8	3	1	5	17	4	28	0	-1	1	34	14	56
Huizhou	29	25	42	13	5	24	7	2	9	37	8	47	1	-2	4	87	38	127
Shaoguan	0	0	0	0	0	0	0	0	0	1	0	1	0	0	0	1	0	2
Zhongshan	2	1	2	1	0	1	0	0	0	2	0	2	0	0	0	4	2	6
Jieyang	0	0	0	0	0	0	0	0	0	0	0	0	0	0	0	0	0	0
Meizhou	1	1	1	0	0	1	0	0	0	1	0	2	0	0	0	2	1	4
Shanwei	4	4	6	2	1	4	2	0	3	8	2	13	0	0	1	16	6	26
Yunfu	8	7	11	4	1	7	3	1	5	14	3	23	0	-1	1	28	11	46
Yangjiang	10	8	14	4	2	8	3	1	4	17	4	27	0	-1	1	34	14	55
Qingyuan	6	5	8	3	1	5	1	0	2	7	2	9	0	0	1	17	7	25
Maoming	0	0	0	0	0	0	0	0	0	0	0	1	0	0	0	1	0	1
Hong Kong	47	41	69	21	7	37	22	7	32	46	10	64	10	-20	44	146	46	248
Macao	1	1	1	0	0	1	0	0	0	1	0	1	0	0	0	2	1	3
<b>Total</b>	<b>347</b>	<b>303</b>	<b>511</b>	<b>162</b>	<b>54</b>	<b>289</b>	<b>92</b>	<b>31</b>	<b>131</b>	<b>424</b>	<b>92</b>	<b>519</b>	<b>20</b>	<b>-41</b>	<b>90</b>	<b>1044</b>	<b>439</b>	<b>1540</b>

Table S7 Avoided premature mortality associated with long-term (chronic) exposures to ship-related O<sub>3</sub> due to implementing the ECA.

City	CVD			RES			IHD			TOTAL		
	Mean	95%CI: low	95%CI: up	Mean	95%CI: low	95%CI: up	Mean	95%CI: low	95%CI: up	Mean	95%CI: low	95%CI: up
Guangzhou	22	5	37	3	1	4	11	2	19	26	6	40
Shenzhen	29	6	47	4	1	5	14	3	24	33	7	52
Foshan	4	1	7	1	0	1	2	0	4	5	1	8
Zhuhai	1	0	2	0	0	0	1	0	1	2	0	3
Jiangmen	2	1	4	0	0	0	1	0	2	3	1	4
Dongguan	19	4	31	3	1	3	9	2	16	22	5	35

Zhaoqing	10	2	17	1	0	2	5	1	9	12	3	19
Heyuan	6	1	9	1	0	1	3	1	5	6	1	10
Huizhou	2	1	4	0	0	0	1	0	2	3	1	5
Shaoguan	1	0	2	0	0	0	1	0	1	1	0	2
Zhongshan	1	0	1	0	0	0	0	0	1	1	0	1
Jieyang	0	0	1	0	0	0	0	0	0	0	0	1
Meizhou	3	1	5	0	0	1	1	0	2	3	1	5
Shanwei	2	0	4	0	0	0	1	0	2	3	1	4
Yunfu	6	1	10	1	0	1	3	1	5	7	2	11
Yangjiang	5	1	8	1	0	1	2	0	4	6	1	9
Qingyuan	7	2	12	1	0	1	3	1	6	8	2	13
Maoming	0	0	0	0	0	0	0	0	0	0	0	0
Hong Kong	1	0	2	1	0	1	1	0	1	2	0	3
Macao	0	0	1	0	0	0	0	0	0	0	0	1
Total	125	27	204	18	5	22	60	12	103	143	32	226